

University of Southern Queensland
Faculty of Health, Engineering & Sciences

**Real-time Pollen Detection by Intrinsic Protein
Fluorescence**

A dissertation submitted by

Jonathon Straker

in fulfilment of the requirements of

ENG4112 Research Project

towards the degree of

Bachelor of Electrical & Electronic Engineering (Honours)

Submitted: October, 2020

Abstract

This project seeks to provide a theoretical and experimental foundation for the development of a low-cost sensor system that can be easily deployed in a variety of situations to indicate when conditions are conducive to the development of thunderstorm asthma epidemics.

Thunderstorm asthma epidemics are a relatively rare phenomenon that occurs when a thunderstorm deposits large amounts of pollen on a city or other densely populated area. Events of this type usually result in numerous people suffering from acute onset asthmatic symptoms, with many requiring subsequent medical treatment.

To determine the most viable option for the design of the sensor system an extensive literature review was conducted, and the findings evaluated. From this research, it was established that the most suitable approach was to use fluorescent spectroscopy techniques targeting the intrinsic fluorophores present within the pollen grains. The aromatic amino acids tryptophan and tyrosine are of interest due to strong emissions with absorption maxima within the wavelength achievable with UV LED technology and emission maxima within the spectral sensitivity range of silicon photomultipliers. To this end, the project aims to demonstrate the viability of using protein fluorescence for pollen detection.

A prototype sensor was constructed using readily available materials and tested using multiple pollen grains (20-30) with satisfactory results. Additional experimental tests to establish the single-particle sensing characteristics of the sensor was successful with the detection of a single hibiscus pollen grain (20 μ m) noted.

The results of the experiments showed that ultraviolet light-induced fluorescence targeting tryptophan is a viable means of detecting pollen and could be a suitable technique to use for the development of the pollen sensing system.

University of Southern Queensland
Faculty of Health, Engineering & Sciences

ENG4111/2 *Research Project*

Limitations of Use

The Council of the University of Southern Queensland, its Faculty of Health, Engineering & Sciences, and the staff of the University of Southern Queensland, do not accept any responsibility for the truth, accuracy or completeness of material contained within or associated with this dissertation.

Persons using all or any part of this material do so at their own risk, and not at the risk of the Council of the University of Southern Queensland, its Faculty of Health, Engineering & Sciences or the staff of the University of Southern Queensland.

This dissertation reports an educational exercise and has no purpose or validity beyond this exercise. The sole purpose of the course pair entitled “Research Project” is to contribute to the overall education within the student’s chosen degree program. This document, the associated hardware, software, drawings, and other material set out in the associated appendices should not be used for any other purpose: if they are so used, it is entirely at the risk of the user.

Dean

Faculty of Health, Engineering & Sciences

Certification of Dissertation

I certify that the ideas, designs and experimental work, results, analyses and conclusions set out in this dissertation are entirely my own effort, except where otherwise indicated and acknowledged.

I further certify that the work is original and has not been previously submitted for assessment in any other course or institution, except where specifically stated.

JONATHON STRAKER

██████████

Acknowledgments

I would like to thank my supervisor Dr John Leis for his wisdom and support which help me to realise the successful completion of the project. I would also like to acknowledge the help and support of my family whose understanding and patience enabled me to dedicate the necessary time required to succeed in my studies.

JONATHON STRAKER

Contents

Abstract	i
Acknowledgments	vii
List of Figures	xiii
List of Tables	xv
Chapter 1 Introduction	1
1.1 Overview	1
1.2 Background	1
1.3 Melbourne Thunderstorm Asthma Epidemic	2
1.4 Problem Statement	2
1.5 Ideation	2
1.6 Project Aim	3
1.7 Project Objectives	3
1.8 Project Limitations	4
1.9 Project Consequences	4

1.10	Dissertation Overview	5
Chapter 2 Literature Review		7
2.1	Chapter Overview	7
2.2	Thunderstorm Asthma	7
2.2.1	Causes	8
2.2.2	Prevalence	10
2.2.3	Pollen Counting	12
2.3	Pollen	13
2.3.1	Structure	14
2.3.2	Size	14
2.3.3	Composition	16
2.3.4	Physical Properties	17
2.4	Bio-aerosol Detection Methods	17
2.4.1	Definition	17
2.4.2	Optical	18
2.4.3	Non-optical	22
2.5	Chapter Summary	24
Chapter 3 Methodology		25
3.1	Chapter Overview	25
3.2	Literature Review Analysis	25

3.2.1	Pollen	25
3.2.2	Pollen Detection Criteria	26
3.2.3	Detection Techniques Analysis	26
3.3	Conceptual System Design	29
3.3.1	Evaluation of the Sensing Techniques	29
3.4	Fluorescent Spectroscopy	30
3.4.1	Intrinsic Protein Fluorescence	31
3.4.2	Fluorescent Spectrometer	33
3.5	Chapter Summary	36

Chapter 4 System Design and Experimental Verification of Concepts 37

4.1	Chapter Overview	37
4.2	System Design	37
4.2.1	Component Selection	37
4.3	Initial Testing of the Silicon Photomultiplier	40
4.3.1	Fluorescent Light Flicker	40
4.3.2	Dark Current Measurement	41
4.4	Verification of Tryptophan Fluorescence	42
4.5	Pollen	44
4.6	Phase 1: Fluorescence of Multiple Pollen Grains	46
4.7	Phase 2: Verification of Photobleaching	48
4.8	Phase 3: Fluorescence of a Single Pollen Grain	52

4.9 Chapter Summary	54
Chapter 5 Conclusions and Further Work	55
5.1 Conclusions	55
5.2 Further Work	56
References	57
Appendix A Project Specification	63
Appendix B Risk Assessment	67
B.1 Introduction	68
B.2 Risk Assessment	68
Appendix C Schematic of Proposed Transimpedance Amplifier	72
Appendix D Data Sheet: SensL C-Series SiPm	75

List of Figures

2.1	Pollen grain ruptured by osmotic shock	8
2.2	Proposed mechanism for thunderstorm asthma	9
2.3	Simplified model of the human respiratory tract	10
2.4	Hirst volumetric particle trap	12
2.5	Pollen from pollen trap	13
2.6	Anatomy of a flower	13
2.7	Pollen grain size comparison	15
2.8	Diagram of a proposed automatic optical particle sensor	18
2.9	FTIR Spectrometer major components	19
2.10	Laser scattering	20
2.11	Fluorescent Spectrometer	21
2.12	Fluorescent spectra aromatic amino acids	21
2.13	Capacitive Sensor	22
2.14	Time of Flight Mass Spectrometer major components	23
3.1	Intrinsic biochemical fluorophores	31

3.2	Absorption and emission spectra of the fluorescent amino acids	32
3.3	Fluorescent Spectrometer	33
4.1	Spectrum of the UV Light Source	38
4.2	SiPM PDE versus Wavelength	39
4.3	Optical Bandpass Filter Transmission	39
4.4	SiPM Test Circuit	40
4.5	Fluorescent Light Flicker	41
4.6	Dark Box	42
4.7	SiPM Ambient Light Reading	43
4.8	Tryptophan Fluorescence	44
4.9	Hibiscus Flower	45
4.10	Hibiscus Pollen	45
4.11	Experimental Configuration	46
4.12	Hibiscus Pollen Sample	47
4.13	SiPM Dark Current	50
4.14	Photobleaching Tryptophan Sample	50
4.15	Irradiation of Blank Slides	51
4.16	Photobleaching of Pollen Samples	51
4.17	Single Pollen Particle Detection	53

List of Tables

- 2.1 Worldwide thunderstorm asthma events (excluding Australia) 11
- 2.2 Australian thunderstorm asthma events 11
- 2.3 Pollen size guide 16

- 3.1 Sensing techniques evaluation matrix 30

- 4.1 Voltage readings from irradiated pollen for each run. 47

- B.1 Risk Matrix 68
- B.2 Description of consequences 68
- B.3 Description of likelihoods 69
- B.4 Description of likelihoods 70

Nomenclature

Acronyms

AC Alternating Current

AUD Australian Dollars

FFT Fast Fourier Transform

FTIR Fourier Transform Infrared [Spectroscopy]

IR Infrared

LED Light Emitting Diode

PMT Photomultiplier Tube

SiPM Silicon Photomultiplier

UV Ultraviolet

UVA Ultraviolet 315–400 nm

UVB Ultraviolet 280–315 nm

UVC Ultraviolet 100–280 nm

VUV Vacuum Ultraviolet 10–200 nm

SI Units

μm micrometers

nm nanometer

$^{\circ}\text{C}$ Degrees Celcius

Chapter 1

Introduction

1.1 Overview

This dissertation aims to provide a theoretical and experimental framework to enable the development of an easily deployable real-time pollen sensing system that can be used to provide a continuous count of airborne pollen particles to enable advanced warning of potential thunderstorm asthma epidemics.

1.2 Background

Thunderstorm induced asthma is a potentially life-threatening condition that can not only affect people susceptible to allergic rhinitis but can also affect people who would normally be asymptomatic or mildly symptomatic to airborne pollen. Epidemic levels of thunderstorm asthma occur when a thunderstorm deposits substantial amounts of pollen onto a large population centre and has the potential to overwhelm emergency services and hospitals with large numbers of people presenting with asthma like symptoms. Moreover, thunderstorm induced asthma epidemics have been reported worldwide (Losappio, Heffler, Contento, Falco, Cannito & Rolla 2012).

1.3 Melbourne Thunderstorm Asthma Epidemic

An epidemic thunderstorm asthma event of unprecedented scale and severity struck Melbourne Australia on November 21, 2016 as a storm front moved across the city between 1700h and 1830h AEDT and deposited a large amount of rye grass pollen on the densely populated urban areas. Over the next 2 days around 3500 patients inundated local hospital emergency departments exhibiting asthma like symptoms. From the 3500 presentations 35 admissions to intensive care were made with 9 subsequent deaths (Lee, Kronborg, O’Hehir & Hew 2017). Interestingly, a substantial number of the people who were affected reported being outdoors between 1700h and 2000h after the thunderstorm had passed (Lee et al. 2017). It was also noted that that many of the people presenting to emergency departments had never experienced asthma symptoms before (Guest 2017). Subsequent studies and analysis of the thunderstorm asthma epidemic revealed that rye grass pollen was a major causal factor in the epidemic with pollen traps recording over 100 grains/m³ on the 21st of November.

1.4 Problem Statement

Problem Statement Pollen measurement and forecasting technologies and techniques available at the time of the Melbourne thunderstorm asthma epidemic failed to predict the occurrence and severity of the event. Moreover, the pollen counting stations that were operational around Melbourne were not able to provide real-time pollen counts to alert emergency services and susceptible people of the impending risks.

1.5 Ideation

Considering the events of the 2016 Melbourne thunderstorm asthma epidemic it is evident that a need exists for a reliable network of real-time pollen monitoring sensors that can provide a timely warning of conditions which are conducive to thunderstorm asthma epidemics. If a sensor network could be deployed around population centres real-time pollen counts and meteorological data could be combined to provide warnings and im-

prove forecasting techniques. This information could be used to alert emergency services of a possible thunderstorm asthma epidemic event occurring and to prepare accordingly. Additionally, susceptible people could also use this information to seek shelter and minimise exposure to the allergens. While there are several sensor systems and techniques that can be employed to detect airborne particle like pollen, generally these systems are expensive, complex, and require a time consuming laboratory analysis. These factors make such systems not readily able to be adapted for continuous sampling of allergens in metrological stations. What is required is a cost-effective sensor system that is reliable, low maintenance, with high availability that can reliably detect single grains of pollen continuously in all weather conditions.

1.6 Project Aim

The goal of this work is to provide an initial investigation into the practicality of developing a low cost easily deployable automatic pollen sensing system that utilises commercially available materials and equipment.

1.7 Project Objectives

1. Conduct a literature review to aid in the understanding of thunderstorm induced asthma, the physical and chemical composition of pollen, and to research various sensing techniques that could be employed for real-time pollen detection in outdoor metrological stations.
2. Determine the most practical sensing techniques to use for the sensing system considering limited resources.
3. Design and build a prototype sensor.
4. Collect pollen samples and test the sensor with real pollen (static sample).
5. Determine the sensor's optimal operational parameters with the goal of single particle detection.
6. Redesign the sensor system with the information collected from objective 5.

7. Using the collected pollen samples test the sensitivity of the sensor to determine if single particle detection is feasible.

1.8 Project Limitations

This project is intended to investigate and deliver the foundational knowledge and experimental observations necessary to determine the feasibility of the chosen sensing technique and does not intend to deliver a fully functional calibrated instrument ready for use.

1.9 Project Consequences

In considering the events of the Melbourne thunderstorm asthma epidemic it is reasonable to assume that had a timely warning been raised alerting the people of Melbourne and surrounding areas to the high pollen counts that many people could have taken precautions to avoid unnecessary exposure to the airborne allergens. This could have resulted in fewer people needing to seek assistance from emergency services and hospitals for severe acute asthmatic symptoms. It is hoped that this project may provide the impetus for the development of a low-cost sensor network that could be deployed widely around population centres. Given the scale of the Melbourne epidemic, the burden of disease (thunderstorm asthma) to the community should not be underestimated. A system that could provide advanced warning of abnormal conditions could have significant public health benefits.

1.10 Dissertation Overview

This dissertation is organized as follows:

Chapter 1 Introduction to the topic, background information na project ideation.

Chapter 2 Literature review to examine pollen and bio-aerosol sensing techniques with an emphasis on methods that could be used to develop miniaturised sensor systems with commercially available components.

Chapter 3 Examination, and evaluation of sensing methods and practices to deliver a functional prototype.

Chapter 4 System design considerations and experimental verification of concepts and sensor performance.

Chapter 5 Conclusion and Further Work.

Chapter 2

Literature Review

2.1 Chapter Overview

The purpose of this literature review is to provide the necessary theoretical knowledge to identify the most suitable sensing technique that could be employed in the development of the pollen sensing system. This chapter aims to provide an overview of the current state of research into thunderstorm induced asthma, pollen, and techniques for the detection of bio-aerosol particles.

2.2 Thunderstorm Asthma

Thunderstorm asthma epidemics are events that describe the occurrence when numerous people (in a localised or widespread geographic area) experience sudden onset asthmatic symptoms during or shortly after a thunderstorm has passed through the area. Typically, symptoms can vary from mild to severe and can affect people that would not normally be predisposed to asthma. It has also been noted that people that are outside during or shortly after the thunderstorm has passed are more likely to experience symptoms (Lee et al. 2017). Furthermore, thunderstorm asthma events have the potential to overwhelm emergency services and hospitals with a sudden influx of people experiencing mild to severe asthmatic symptoms (Lee et al. 2017).

2.2.1 Causes

The causal mechanism for thunderstorm induced asthma is not well understood, but it is believed to be produced by the generation of allergenic aerosol particles by thunderstorms which can result in 2 ways (D'Amato, Liccardi & Frenguelli 2007). When a thunderstorm is forming over an area of land that has numerous flowering plants the thunderstorm up-draughts can pick up a significant amount of pollen and suspend this material within the storm cloud. As the pollen enters the cloud, hydration occurs and the pollen grains rupture by osmotic shock causing the inner material of the pollen to exude through the pollen wall and release allergenic cytoplasmic starch granules which are typically 0.9–1.7 μm in size (D'Amato et al. 2007). These allergenic particles remain in the thunderstorm until brought to the ground by downdraughts (Beggs 2017).



Figure 2.1: Pollen grain ruptured by osmotic shock (D'Amato et al. 2007).

An extension of this effect is the nucleation of small water droplets around the bio-aerosols of the ruptured pollen grains. These small water drops coalesce to form raindrops within the thunderstorm (Beggs 2017). As the rain starts to fall the allergenic nucleus of the raindrop are carried to the ground where the formation of the allergenic aerosol occurs.

When the raindrop hits a solid object, the drop dissipates and subsequently releases the piece of ruptured pollen as an aerosol particle.

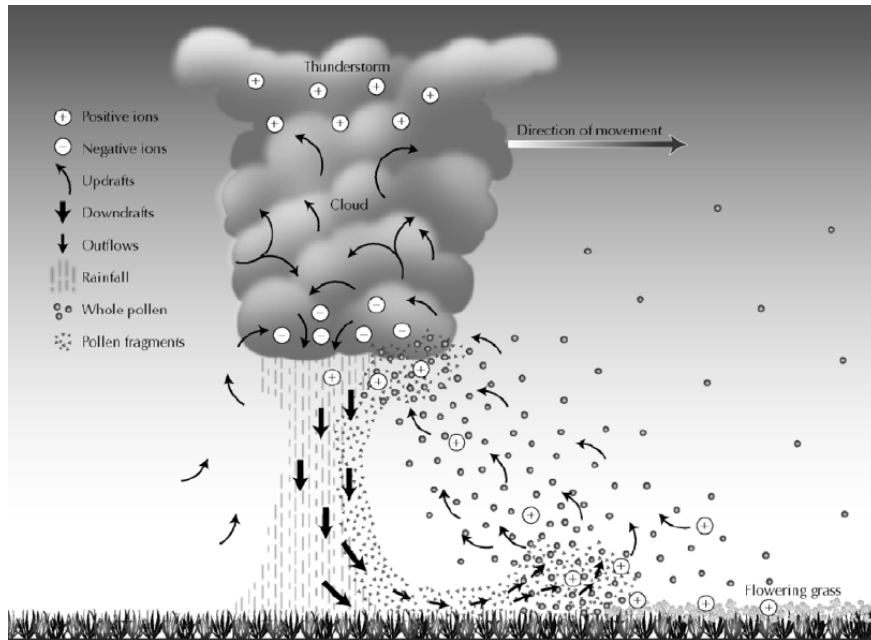


Figure 2.2: Proposed mechanism for thunderstorm asthma (Guest 2017).

Due to the small size of the aerosol particle, they can be inhaled into the airways much deeper than a full grain of pollen. Typically, as pollen grains are greater than $10\ \mu\text{m}$ in diameter, the grains generally do not enter the bronchial region of the airways and are confined to the upper respiratory tract (D'Amato et al. 2007). Conversely, as the cytoplasmic particles of ruptured pollen grains of the order of $2.5\ \mu\text{m}$ in diameter, these particles can enter the bronchial regions of the lower respiratory tract and induce asthma like symptoms (D'Amato et al. 2007).

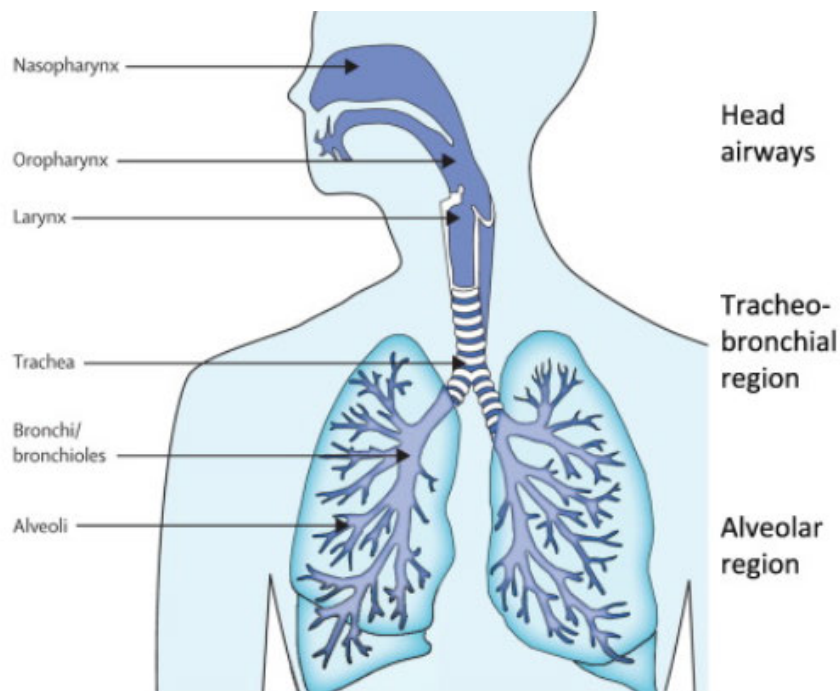


Figure 2.3: Simplified model of the human respiratory tract (Fröhlich-Nowoisky et al. 2016).

2.2.2 Prevalence

Thunderstorm asthma epidemics have been noted worldwide with events having been recorded in Europe, North America, the Middle East, and Australia. Table 2.1 lists all reported occurrence worldwide (excluding Australia) and Table 2.2 lists the reported Australian events (Harun, Lachapelle & Douglass 2019).

Table 2.1: Worldwide thunderstorm asthma events (excluding Australia)

Location	Date	Presentation to ED	Preposed allergen trigger
UK, Birmingham	1983, July	106	Fungal Spores
UK, Nottingham	1984, June	19	Fungal Spores
UK, Leicester	1989, July	32	Fungal Spores
UK, London	1994, June	640	Grass Pollen
Canada, Calgary	2000, July	157	Fungal Spores, Pollen
UK, Cambridge	2002, July	57	Fungal Spores
Saudi Arabia, Al-Khobar	2002, November	NS	NS
Italy, Naples	2004, June	7	Pollen
UK, South-East England	2005, June	0 (none to ED)	NS
Italy, Puglia	2010, May	20	Olive Pollen
UK, London	2013, July	40	NS
Iran, Ahvas	2013, November	>2000	NS

Abbreviations: ED, Emergency Department; NS, Not Specified

Table 2.2: Australian thunderstorm asthma events

Location	Date	Presentation to ED	Preposed allergen trigger
Melbourne	1984, November	85	NS
Melbourne	1987, November	154	NS
Melbourne	1989, November	277	Grass Pollen
Tamworth	1990, November	110	Grass Pollen
Wagga Wagga	1997, October	215	Grass Pollen
Newcastle	1998, October	6	Grass Pollen
Melbourne	2003, November	70	Grass Pollen
Melbourne	2010, November	36	Grass Pollen
Melbourne	2011, November	30	Grass Pollen
Canberra	2014, October	15	Grass Pollen
Melbourne	2016, November	>3400	Grass Pollen

Abbreviations: ED, Emergency Department; NS, Not Specified

While the tables list major events of thunderstorm asthma, it is likely that many smaller scale events are under-reported. Studies of asthma related emergency room visits following thunderstorms have been conducted in both the US and Canada with the US study show-

ing a 3% increase in emergency room presentations post-thunderstorm with the Canadian study showing a 35% increase in emergency room presentations post thunderstorm during summer months (Harun et al. 2019).

2.2.3 Pollen Counting

Currently pollen counting and forecasting relies heavily on the use of particle traps and optical microscopy. Particle traps generally employ an adhesive substance on a rod, drum, or slide which is rotated or moved periodically to expose a new area of the adhesive material to allow for the concentration at a given time to be established. The Hirst particle trap is a typical device of this type that is deployed at pollen counting stations to collect airborne pollen sample for identification and counting (Blank, Vinayaka, Tahir, Vellekoop & Lang 2015).

In the Hirst trap figure 2.4 air is draw in at (2) and the particle adhere (1) to the recording drum (3). An air pump (5) creates a continuous flow of air across the recording drum.

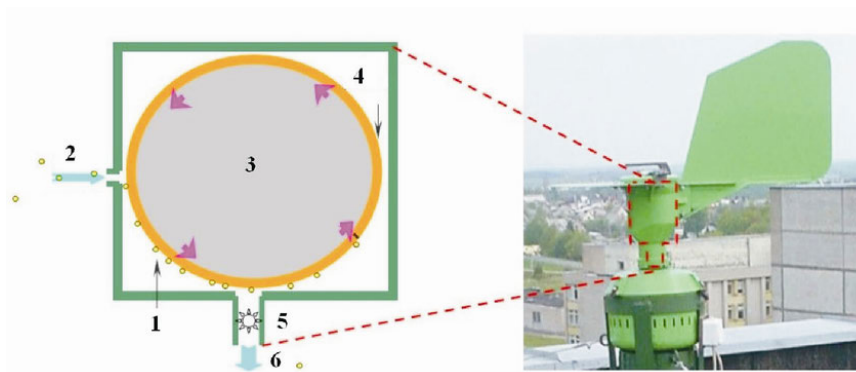


Figure 2.4: Hirst volumetric particle trap (Fröhlich-Nowoisky et al. 2016).

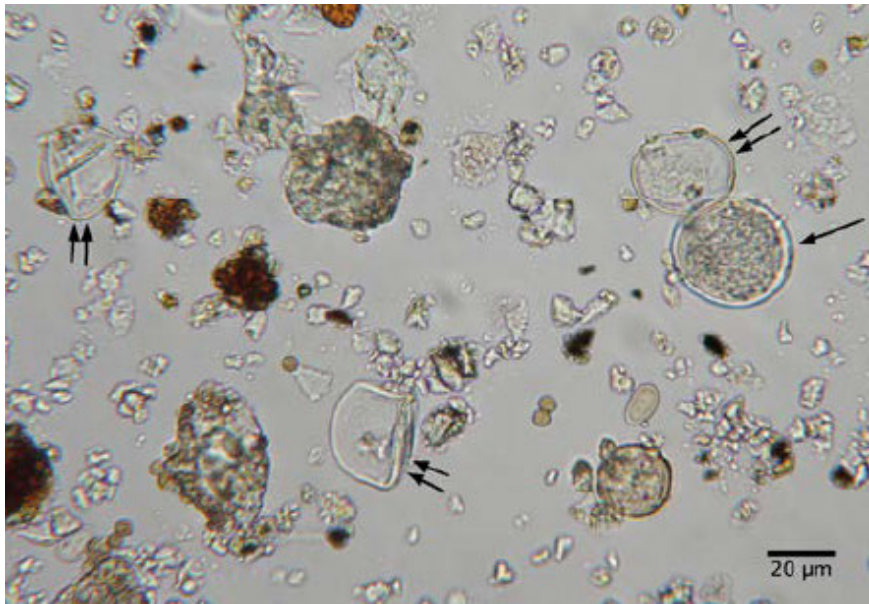


Figure 2.5: Microscopy image of samples taken from a pollen trap in Melbourne at 6:30pm on the 21 November 2016. Double arrows shows ruptured pollen grains with single arrow for intact pollen grains (Guest 2017).

2.3 Pollen

Pollen is a fine-grained organic material produced by flowers and is used in the plants reproductive cycle. The pollen is produced in the flower's stamen by the anther where the pollen sac is located (Eyde 2020). The purpose of the pollen is to transfer the flowers male gametes (sperm cells) to a flowers stigma where the pollen will germinate and fertilise the flower possibly resulting in seed or fruit generation (Eyde 2020).

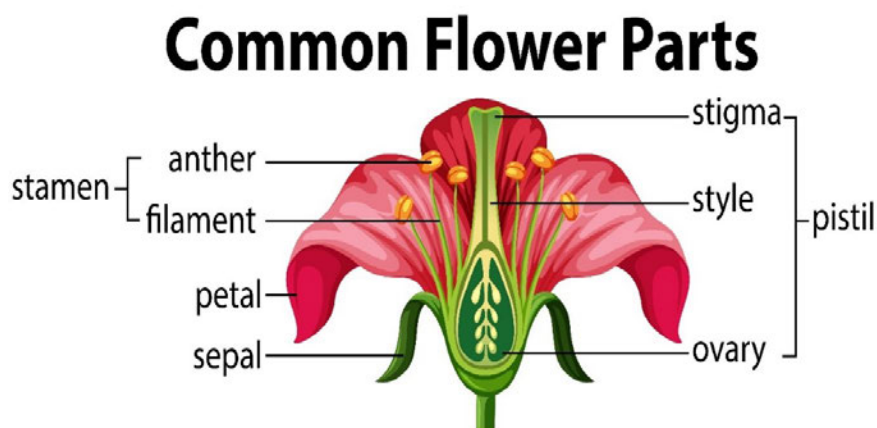


Figure 2.6: Anatomy of a flower (brgfx 2020).

2.3.1 Structure

Pollen generally, has a double-wall structure that encapsulates the pollen's cytoplasm where the semen is present (Quilichini, Grienberger & Douglas 2015). The outer wall is made of the outer exine and inner intine layers which protects the semen from solar radiation and other environmental factors (Halbritter, Ulrich, Grímsson, Weber, Zetter, Hesse, Buchner, Svojtka & Frosch-Radivo 2018). The exine is comprised mainly of the biopolymer sporopollenin with the intine being comprised of cellulose and pectin (Halbritter et al. 2018). The inner cytoplasm and semen are composed of lipids, proteins, and carbohydrates (Jensen 1968).

2.3.2 Size

Generally, the size of pollen grains is in the range of less than $10\ \mu\text{m}$ (Myosotis) to over $200\ \mu\text{m}$ (Cucurbita) and is dependant on the plant species, hydration levels, and natural variation (Halbritter et al. 2018). Grass pollen (a primary allergenic pollen) normally produces pollen in the size range of $20\text{--}25\ \mu\text{m}$ (Sporomex 2020). A sample of different pollen and associated sizes is shown in figure 2.7 and table 2.3 (Sporomex 2020).

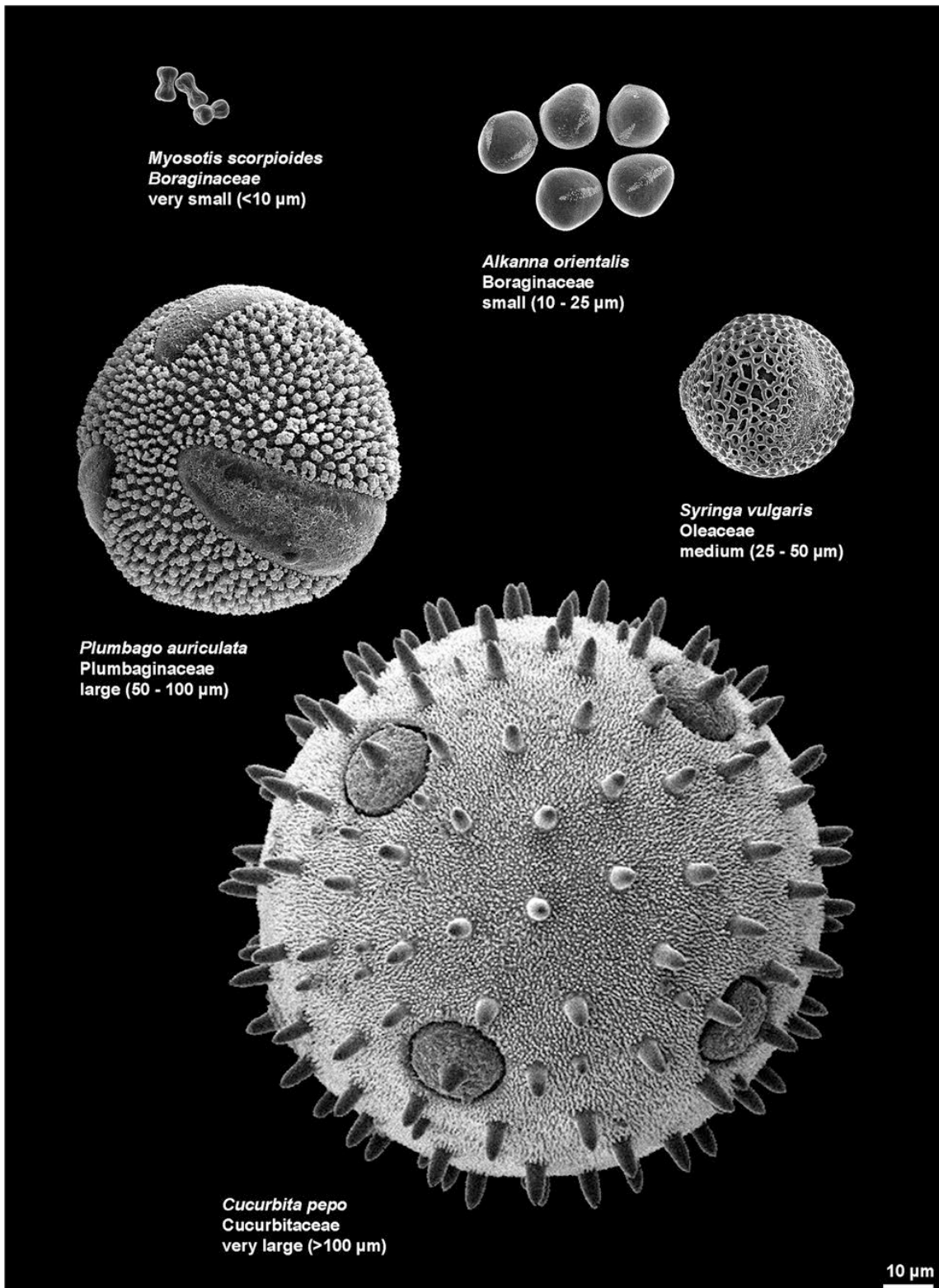


Figure 2.7: Pollen grain size comparison (Halbritter et al. 2018).

Table 2.3: Pollen size guide

Plant Species	Size Range
Myosotis	2.4–5 μm
Penicillium	3–5 μm
Aspergillus niger	4 μm
Cantharellus minor	4–6 μm
Ganoderma	5–6.5 μm
Chlorella Vulgaris	8–10 μm
Oilseed rape	10–12 μm
Agrocybe	10–14 μm
Urtica dioica	10–12 μm
Periconia	16–18 μm
Epicoccum	20 μm
Helianthus annuus	20 μm
Ryegrass	21 μm
Timothy grass	22 μm
Rye	22 μm
Wheat	23 μm
Hemp	24 μm
Lycopodium clavatum	25 μm
Rape hemp	25 μm
Lycopodium powder	40 μm
Rye grass	40 μm
Pine	50 μm
Maize	80 μm
Abies	125 μm
Cucurbitapapo	200 μm
Cuburbita	250 μm

2.3.3 Composition

As an organic material pollen is not comprised of one unique substance, but is a combination of many different organic molecules. Pollen contains water, carbohydrates, proteins, minerals, vitamins, unsaturated fats, and saturated fats (LILEK, GONZALES, BOŽIČ, BOROVŠAK & BERTONCELJ 2015). Pollen also contains the essential amino acids valine, methionine, histidine, lysine, threonine, isoleucine, leucine, arginine, and the aro-

matic amino acids phenylalanine, tyrosine, and tryptophan which are all present in pollen (Somerville 2001). Additionally, most of the amino acids in pollen are contained in the outer exine layer of the shell (LILEK et al. 2015). This project will be concerned with the aromatic amino acid tryptophan which is reported to have levels in pollen of between 0.028 g/kg to 0.197 g/kg (LILEK et al. 2015). Furthermore, the composition of pollen is highly variable with season, region, country, and species all contributing to variations of chemical composition (LILEK et al. 2015).

2.3.4 Physical Properties

Pollen is an extremely stable organic material that is resistant to many acid/alkaline environments and can withstand temperatures of more than 200°C. Pollens are also very elastic and can endure tonnes of pressure without damage (Sporomex 2020).

2.4 Bio-aerosol Detection Methods

The detection and classification of bio-aerosol particles has been a subject of research for over 30 years especially from a military bio-weapons perspective. Broadly, techniques for the detection and classification of bio-aerosol can be divided into two categories optical and no-optical techniques.

2.4.1 Definition

Bio-aerosols are atmospheric particles that are produced by a biological organism and can include fungal spores, plant pollen, algae, bacteria, proteins, viruses, and plant debris. Particle sizes range from 1 nm (proteins) to 100 μm (pollen) (Fröhlich-Nowoisky et al. 2016). The upper size limit for aerosol particle is defined by the particles ability to remain suspended in the air for an extended period.

2.4.2 Optical

Optical systems pertain to those techniques that utilise light from ultraviolet (UV), visible, and infrared (IR) as the main sensing method.

Optical Microscopy

Optical microscopy involves schemes that capture the bio-aerosol particles on a filter or adhesive media and where a trained operator uses a light microscopy to physically look at the particles for identification and counting (Blank). While this technique produces excellent results for pollen identification, the process is slow as filters or adhesive media are only checked at given interval e.g. daily (Blank et al. 2015). Attempts are being made to automate the process using image classification techniques (machine learning) but currently are achieving approximately 80% accuracy in identification (Kadaikar, Guinot, Trocan, Amiel, Conde-Cespedes, Oliver, Thibaudon, Sarda-Estève & Baisnée 2019). Furthermore, schemes for the continuous sampling of particles using robotic microscopy assemblies like in figure 2.8. Are under development and could potentially provide near real-time pollen counts (Blank et al. 2015).

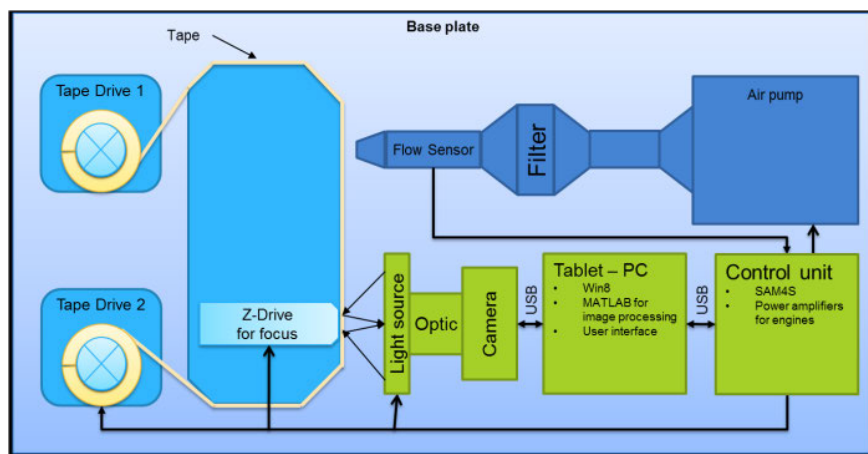


Figure 2.8: Diagram of a proposed automatic optical particle sensor (Blank et al. 2015).

Fourier Transform Infrared Spectroscopy

Fourier transform infrared (FTIR) spectroscopy is a technique that utilises infrared light to obtain the infrared emission and absorption spectra of a given sample either solid, liquid or gas. These spectra can be used to identify the substances present in the sample (Smith n.d.). FTIR spectrometers utilise a polychromatic light source, Michelson interferometer,

pyrolytic sensor, and computer system to process the interferogram into the frequency domain to obtain the spectra.

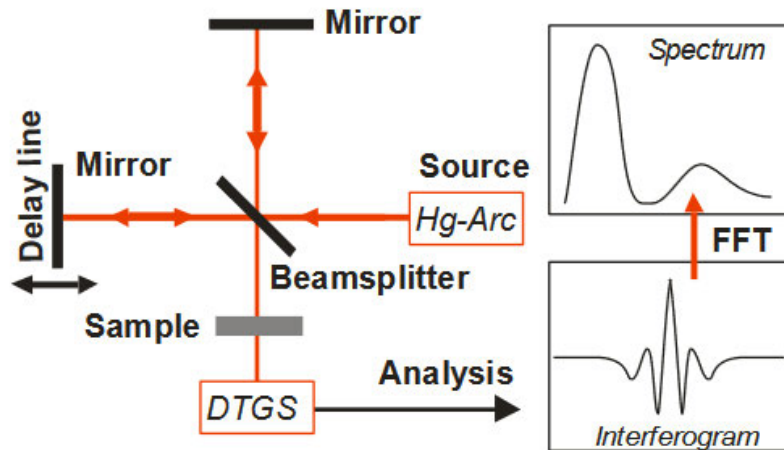


Figure 2.9: FTIR Spectrometer major components (Panowicz et al. 2011).

The FTIR spectrometer works on the principle of scanning through the polychromatic light using the interferometer to continuously select the desired wavelength (within the resolution of the interferometer) of light which is then applied to the sample before going to the detector. The desired wavelength of light is produced by the interference of light (phase difference) caused by the difference in length between the stationary and delay arms of the interferometer and is related to the position of the movable mirror in the delay arm (Smith n.d.). The position of the movable mirror and the intensity information from the detector is used to produce the interferogram. This is then processed back into frequency domain by using an Fast Fourier Transform (FFT) algorithm to produce the desired absorption and emission spectra.

FT-IR spectroscopy can be used to identify the composition of bio-aerosol particles and can also discriminate between different species of plant pollen (Pappas, Tarantilis, Harizanis & Polissiou 2003).

Laser Scattering

The use of laser scattering for particle detection is a well-established technique and can be used to count, size, and identify particles. The process works by irradiating a sample with laser light and measuring the forward, side, and backward scattered light (Shimadzu 2020). This information can be used to measure the particles size, surface, and light absorption characteristics.

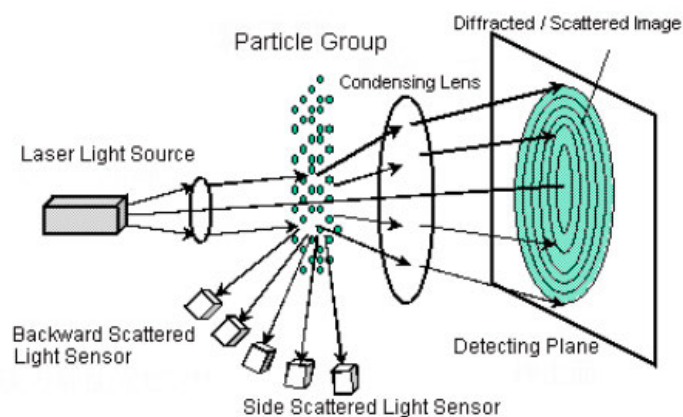


Figure 2.10: Laser scattering (Shimadzu 2020).

The forward scattered light creates a diffraction pattern that is related to the size of the particles being irradiated. Additionally, the intensity of the light measured by the forward detector indicates the light absorption characteristic of the particles. The side and backward scattered light can provide information about the surface reflectivity characteristics of the particle. By combining these measurements, the size and composition of the detected particles can be determined (Kawashima, Clot, Fujita, Takahashi & Nakamura 2007).

Fluorescent Spectroscopy

Fluorescent spectroscopy utilizes the principle of luminescent fluorescence for the detection and measurement of fluorophores (molecules that luminesce fluorescently). Fluorescent luminescence occurs when an atom absorbs a photon which moves an electron in an excited singlet state (the excited electron is paired to an electron in the ground state by opposite spin) and then emits a photon returning the paired electron to the ground state spin (Lakowicz 2007). The wavelength of the emitted photon is generally longer and has lower energy (Stokes shift) than the absorbed photon (Lakowicz 2007). The efficiency of the process (is the ratio of the number of photons absorbed to the number of photons emitted) is called the quantum yield (Lakowicz 2007).

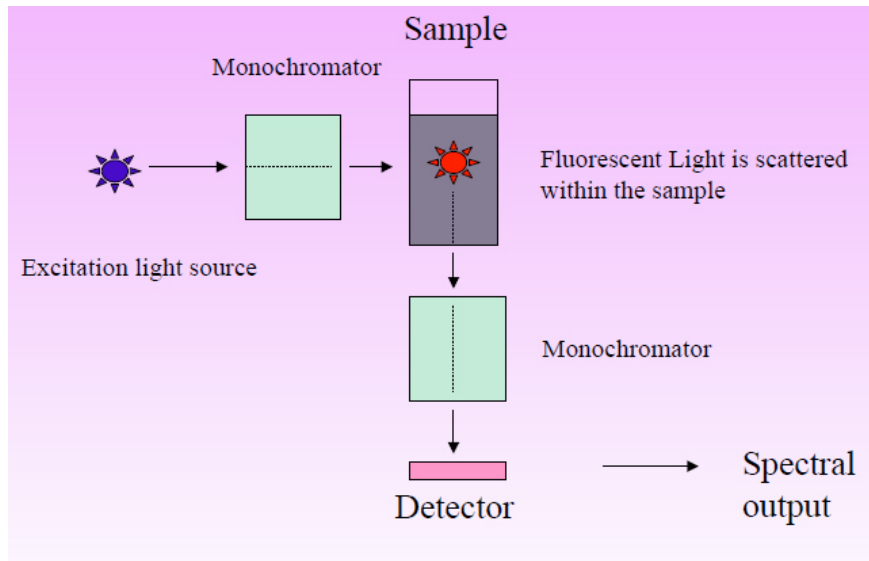


Figure 2.11: Fluorescent Spectrometer major components

(Panowicz et al. 2011).

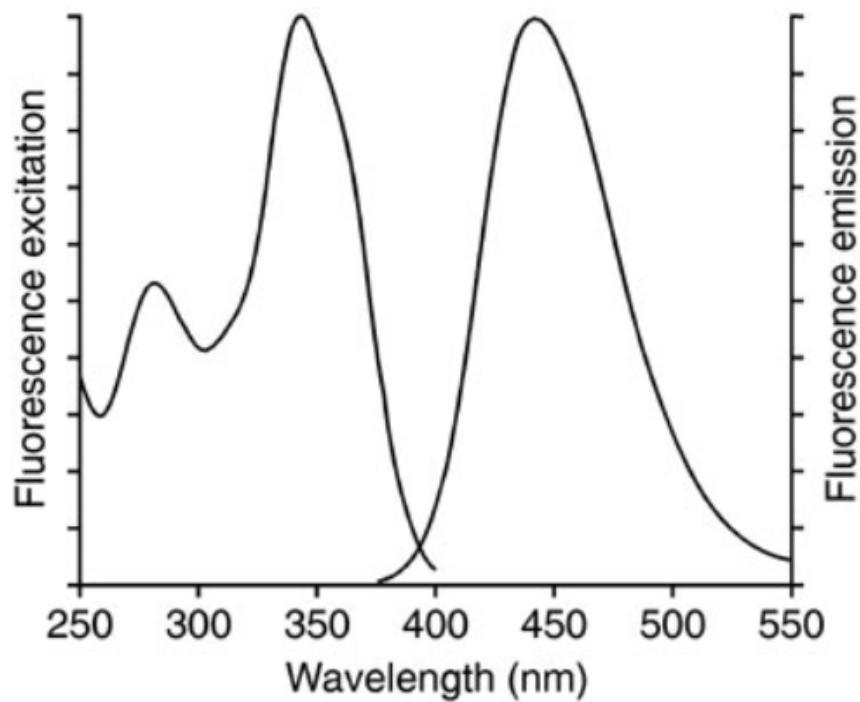


Figure 2.12: Fluorescent spectra: excitation (left) emission (right) (Hooijschuur 2020).

Fluorescent spectrometers are relatively simple and work by irradiating the desired sample with monochromatic light followed by the detection of the resulting emissions from the sample. The light source can be either polychromatic and employ a monochromator (filter) or can be intrinsically monochromatic. The detector usually employs a monochromator (of a wavelength appropriate to the emissions for the desired molecule) as detectors are

normally sensitive to a wide spectral range (Lakowicz 2007). Fluorescent spectrometers can be constructed to detect only one type of molecule or can employ multiple channels to reliably identify more complex compounds like pollen (Kaliszewski, Włodarski, Młyńczak, Leśkiewicz, Bombalska, Mularczyk-Oliwa, Kwaśny, Buliński & Kopczyński 2016).

2.4.3 Non-optical

Capacitive Sensing

Capacitive based sensor systems use highly sensitive capacitance measuring techniques to detect particles moving through the sensor. These systems rely on the difference in dielectric properties of particulate matter and air. Generally, the relative permittivity of the particle will be greater than the relative permittivity of air and such will interact with the electric field between the sensors electrodes resulting in an increase of capacitance (Carminati, Pedalà, Bianchi, Nason, Dubini, Cortelezzi, Ferrari & Sampietro 2014).

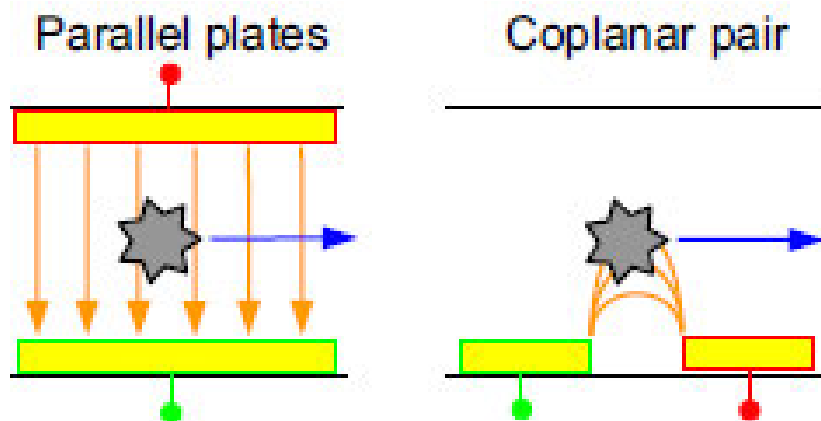


Figure 2.13: Capacitive sensor architecture (Carminati et al. 2014).

A significant advantage of capacitive sensors is the scope for miniaturisation with the possibility of being able to embed sensors of this type into personal portable devices like smart watches (Carminati et al. 2014).

Time of Flight Mass Spectroscopy

Time of flight mass spectrometry is a mass spectroscopy technique that uses time of flight measurements to determine the mass to charge ratio of a particle. As particles are drawn into the spectrometer the particles are accelerated by a partial vacuum before being sized

and velocity measured by scattering lasers. The particles are then desorbed and ionised before entering the ion chamber (Tobias, Schafer, Pitesky, Fergenson, Horn, Frank & Gard 2005). In the ion chambers the ions are subject to a constant electrostatic field which interacts with the ions. The amount of interaction is dependent on the ions charge with ions having a lower mass to charge ratio accelerating more than ions with higher mass to charge ratio (Tobias et al. 2005). Using the information about the initial velocity of the particles and the interactions the particle had with the electrostatic field in the ion chambers, the mass to charge ratio can be determine and hence the chemical composition of the particle.

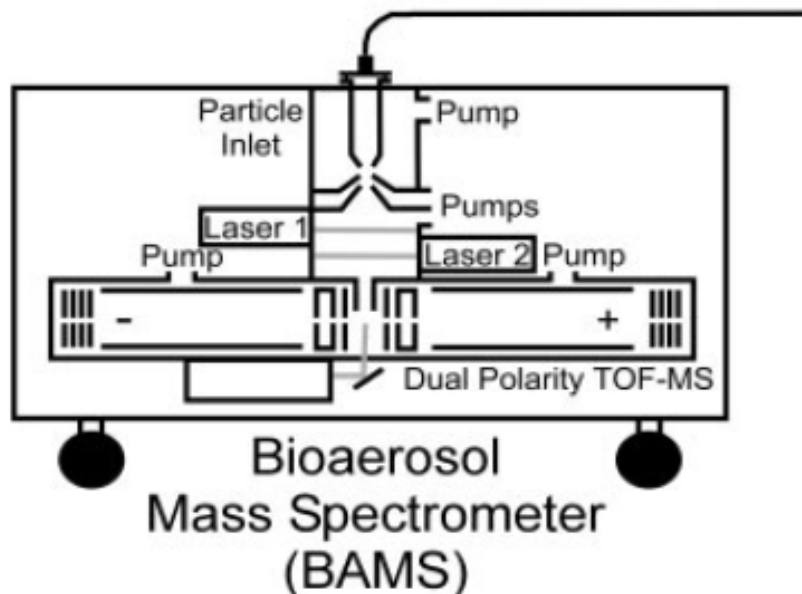


Figure 2.14: Time of Flight Mass Spectrometer major components (Tobias et al. 2005).

2.5 Chapter Summary

A review of the available literature has provided insight into potential sensing techniques that could potentially be exploited for the purpose of detecting airborne pollen particles. These techniques range from automated optical microscopy and laser scattering that can detect the size and shape of particles to analytical chemical techniques like fluorescent spectroscopy, Fourier transform infrared spectroscopy, and time of flight mass spectroscopy that can provide information at the molecular level. Additionally, the chemical and physical characteristics of pollen have also been investigated and will provide a means by which to evaluate the suitability of the sensing techniques for the purpose of this design and provide a direction for the design process.

Chapter 3

Methodology

3.1 Chapter Overview

The purpose of this chapter is to analyse and select an appropriate detection method for the development of the pollen sensing system with the aim of developing a prototype using cost effective commercially available components and materials.

3.2 Literature Review Analysis

The literature review has provided direction for the design process and revealed several important considerations for the sensor system. To initiate the design process an understanding of the chemical and physical composition of pollen is required and will facilitate the evaluation of the suitability of the proposed detection methods established by the literature review.

3.2.1 Pollen

Pollen is a complex organic material that contains many molecules that could be targeted for detection purposes. Carbohydrates, proteins, amino acids, vitamins, and minerals are all present in pollen and can provide a means to discriminate pollen from other airborne particles like carbon or dust. Physically, pollen grain sizes range from approximately

2–200 μm and are found with a variety of surface characteristics and shapes figure 2.3. Furthermore, particles of ruptured pollen are irregular in shape and size with samples of $\leq 1 \mu\text{m}$ in size being noted (Beggs 2017).

3.2.2 Pollen Detection Criteria

Analysis of the literature review has provided the following pollen detection criteria which are intended as a guide to evaluate the proposed sensing techniques.

- Carbohydrates, proteins, and amino acids could be targeted as a detection means to discriminate between organic and inorganic particles.
- Single particle detection of pollen grains $> 2 \mu\text{m}$ on a continuous basis.
- Detection of submicron ruptured pollen is highly desirable.

3.2.3 Detection Techniques Analysis

Evaluation of the selected detection techniques from the literature review against the pollen detection criteria provides insight into the most suitable processes.

Optical Microscopy

Optical microscopy techniques are the current standard detection method and provide high levels of information regarding airborne particles. Automation of this process is being investigated by research organisations and should be able to provide near real-time detection. Optical microscopy techniques and equipment have the following general characteristics.

- Proven technology.
- Good discrimination of particle types.
- Identification of different pollen species possible.
- Requires consumables e.g. adhesive media

- Automated implementation requires precision moving parts e.g. focus mechanisms, tape drives, and optics.
- Slow compared to other techniques.

Fourier Transform Infrared Spectroscopy

Fourier Transform Infrared Spectroscopy is a proven analytical technique that can identify and discriminate between organic and inorganic molecules. The process can achieve single particle detection and can provide additional information about the composition of inorganic particles for air quality monitoring purposes. IR spectroscopy equipment and techniques have the following characteristics.

- Excellent information about particles.
- Identification of different pollen species possible.
- Scan time approximately 1 sec per sample.
- Numerous moving parts and precision optics required.
- Would require some mechanism to capture particles for analysis (adhesive tape, electrostatics).

Laser Scattering

Laser scattering techniques are widely deployed for both particle detection and sizing in gases and liquids. Commercially available instruments of this type are readily available as both sensors and full systems. Back scattering and forward absorption measurements can be made by laser scattering sensor systems which can yield information about the particles composition and help determine if the particle is organic or inorganic. Laser scattering techniques and equipment have the following characteristics Proven established technique for particle detection.

- Fast response.
- Capable of yielding particle size information.
- Detection of surface characteristics by forward absorption, and back scattering

- Potential for the discrimination of biological and non-biological particles.
- Many commercially available particle detectors use this technique.

Fluorescent Spectroscopy

Fluorescent spectroscopy is an established technique for the detection of fluorescent molecules in organic and inorganic materials. Highly sensitive detectors and precision optical filters can achieve single particle detection. Fluorescence spectrometry equipment and techniques have the following characteristics.

- Well established technique for the detection of amino acids.
- No moving parts or precision mechanisms.
- Monochromatic light source required.
- Does not require any consumables.

Capacitive Sensing

Capacitive sensing of airborne particles is possible using either parallel plate or coplanar architectures which could be used to develop compact sensors. Discrimination between organic and inorganic particles maybe achievable. Capacitive sensors have the following characteristics.

- Low cost.
- No moving parts.
- High sensitivity electronic measurement circuitry required.
- Sensor does need periodic cleaning.
- Susceptible to environmental conditions.
- Unknown if this sensor can discriminate effectively between organic and inorganic particles in all environmental conditions.

Capacitive Sensing

Mass spectroscopy is a powerful analytical technique for molecular analysis and could provide high levels of information about airborne particles. Discrimination between organic and inorganic molecules is achievable and pollen species identification could also be realised. Mass spectroscopy equipment and techniques have the following characteristics.

- Excellent ability to gather information about particle composition.
- Complex with many precision parts.
- Trained operator required.

3.3 Conceptual System Design

To create a conceptual system design, several requirements for the sensor system were developed and will provide a means to evaluate the researched detection techniques and are as follows.

- No moving parts except a fan (if possible).
- No precision mechanical/optical mechanisms.
- No consumables.
- Minimum number of optical filters and detectors (1 ideally).
- Low cost components that are commercially available from major electronic supply companies.
- Low maintenance, high availability of service.

3.3.1 Evaluation of the Sensing Techniques

Evaluation of the techniques against the conceptual design criteria was done using the following scheme. If the technique meets the criteria than a score of one is registered. Alternatively, if the technique does not meet the criteria than a score of zero is registered.

The technique with the highest overall score is assumed to be the most suitable for further evaluation. Capacitive and mass spectroscopy techniques were not considered viable for further evaluation due to complexity and issues with building a prototype given limited resources and time.

Table 3.1: Sensing techniques evaluation matrix

Evaluation Matrix		Sensing Techniques			
		Optical	FTIR	Laser	Fluor
Criteria	Moving parts	0	0	1	1
	Precision components	0	0	1	1
	Detectors	1	1	0	1
	Maintenance	1	0	1	1
	Consumables	0	0	1	1
	Cost	1	0	1	1
	Score	3	2	5	6

Selection

Evaluation of the detection methods identified in the literature review suggest that fluorescent spectroscopy is the most viable candidate for the development of a sensor system capable of single particle detection of pollen.

3.4 Fluorescent Spectroscopy

Fluorescent spectroscopy utilizes the principle of luminescent fluorescence for the detection and measurement of fluorophores (molecules that luminesce fluorescently). Fluorescent luminescence occurs when an atom absorbs a photon which moves an electron in an excited singlet state (the excited electron is paired to an electron in the ground state by opposite spin) and then emits a photon returning the paired electron to the ground state spin (Lakowicz 2007). The wavelength of the emitted photon is generally longer and has lower energy (Stokes shift) than the absorbed photon (Lakowicz 2007). The efficiency of the process (the ratio of the number of photons absorbed to the number of photons emitted) is called the Quantum Yield (Lakowicz 2007).

3.4.1 Intrinsic Protein Fluorescence

Intrinsic protein fluorescence results from the essential aromatic amino acids tryptophan (trp), tyrosine (tyr) and phenylalanine (phe) which are present in proteins. Tryptophan is the dominant source of UV emission and absorption in proteins and is the primary target of the investigation (Lakowicz 2007). The 3 aromatic amino acids chemical structure is shown in figure 3.1.



Figure 3.1: Intrinsic biochemical fluorophores (Lakowicz 2007).

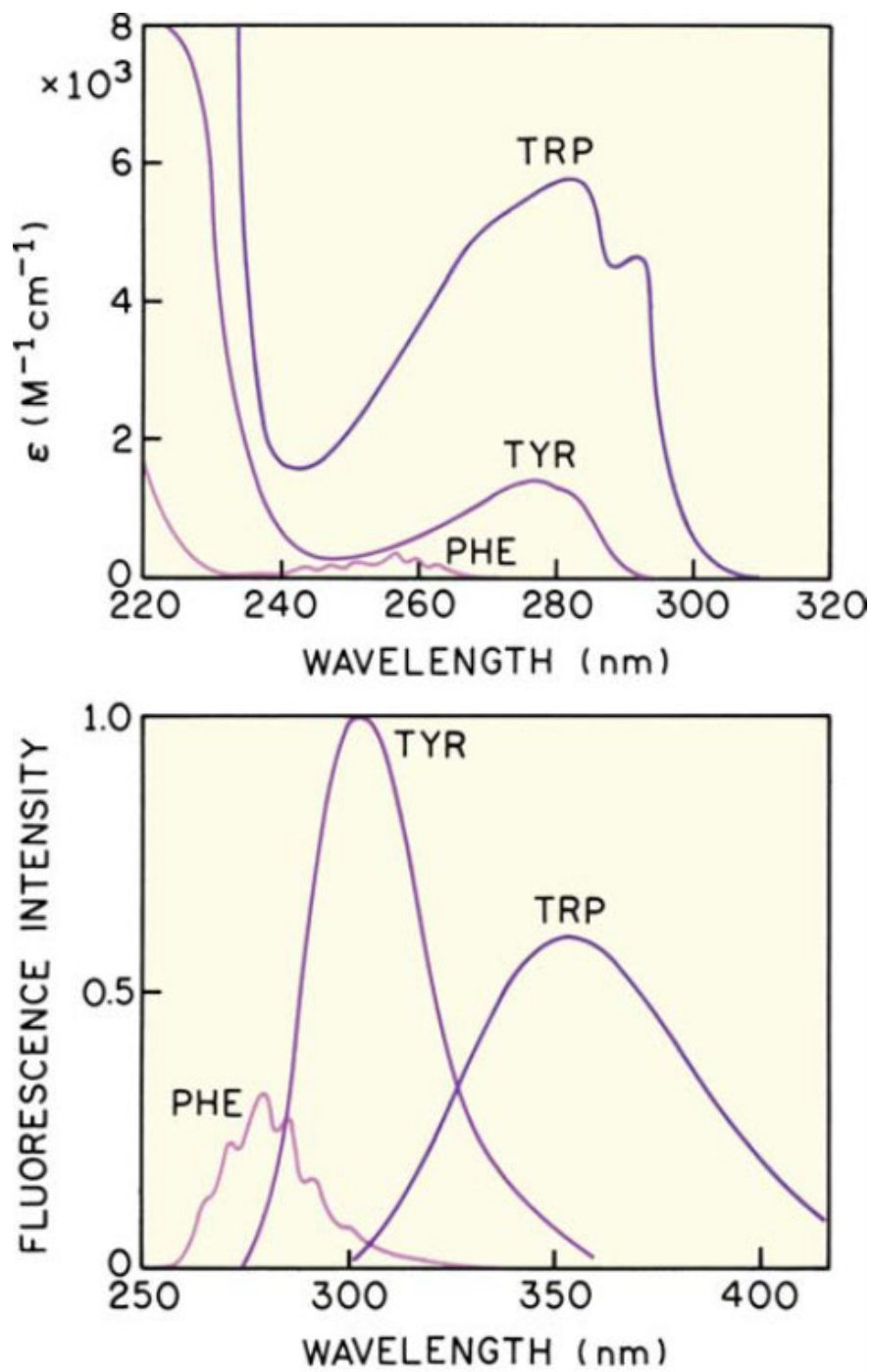


Figure 3.2: Absorption and emission spectra of the fluorescent amino acids in water of pH 7.0 (Lakowicz 2007).

From the absorption and emission spectra in figure 2.11 it can be seen that tryptophan has an absorption peak around 280 nm and emission peak around 350 nm. Additionally, tyrosine also has an absorption peak around 280 nm and an emission peak around 300 nm. Furthermore, these values are only valid for tryptophan dissolved in water as tryptophan is highly sensitive to its local environment with emission shifting resulting from several

phenomena, such as protein unfolding and ligand binding (Lakowicz 2007).

While tryptophan is the primary target molecule, tyrosine could also be detected if a wavelength of 340nm is selected for the detector. This would yield approximately 20% emission intensity for tyrosine and a 50% emission intensity for tryptophan. From this information a sensor system can be tailored to exploit this relationship with an excitation UV light source at 280 nm and a UV sensitive sensor at 340nm.

3.4.2 Fluorescent Spectrometer

At its simplest form, a fluorescent spectrometer is comprised of a monochromatic light source, a monochromator (filter) and a detector which is sensitive to the fluorescent emission wavelength of interest. A simple fluorescent spectrometer is shown in figure 3.3.

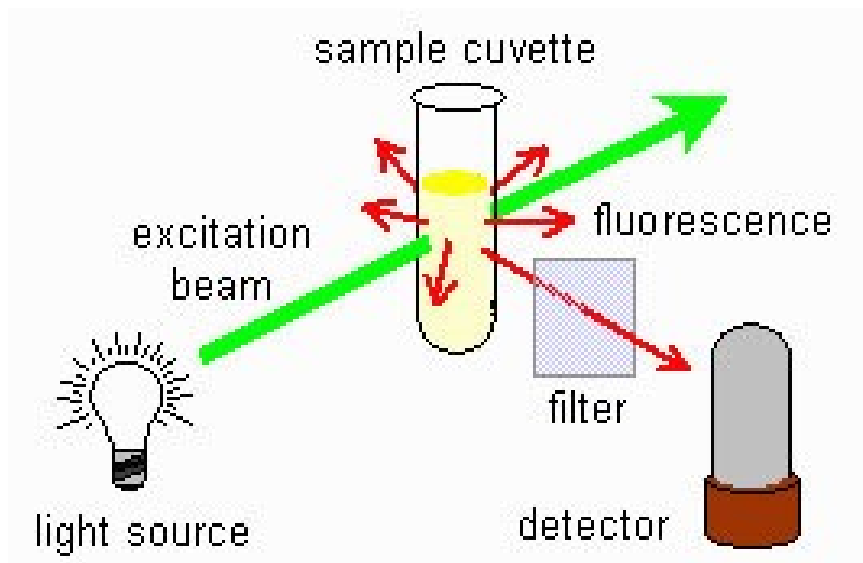


Figure 3.3: Conceptual fluorescent spectrometer (Hooijschuur 2020).

Component Analysis

The selection of individual components will be of critical importance to the performance of the final sensor design. Given the aim of developing a low-cost sensor system performance and cost are the most important metrics to consider when selecting components.

UV Light Source

UV light sources available for this design include UV light emitting diodes (LED), UV

quartz flash lamps, and Excimer lamps. UV flash lamps are Xenon flash lamps with fused quartz envelopes which are transparent to UV light. These lamps have a wide spectral output and would need filtering to be of use in this design (XenonFlashTubes.com 2020). UV Excimer lamps are a discharge lamp and are available in several different configurations with spectral maximums ranging from vacuum ultraviolet (VUV) to ultraviolet A (UVA) (Kogelschatz 2003). As Excimer lamps are monochromatic no additional filtering is necessary resulting in lower construction costs. UV LED's are available in numerous narrow peak spectral wavelengths and power outputs from ultraviolet A (UVA) to ultraviolet C (UVC) and are relatively compact and robust. As the LED's are available with narrow spectral outputs there is no additional need to filter the UV light from the light source resulting in lower design costs. Additionally, it is possible to change the driving current to adjust the light intensity. The advantage of this is that the LED's current draw can be minimised to lower power consumption and reduce heating of the LED prolonging the life of the light source. The selection of a suitable light source was based on ease of use, price, and availability. UV flash and Excimer lamps require ballasts and driving circuitry to operate and are intended for either flash or continuous operation. Alternatively, UV LED's require only a constant current source (for best operation) and can be used either in continuous wave or strobe output. Additionally, UV LED's are easier to acquire with most major electronics supply companies stocking numerous examples. UV flash and Excimer lamps are more specialised and are not as readily available. Based on these metrics UV LED's were selected for the design.

Photodetector

With the primary aim of the research being to perform single particle detection of sub-micron pieces of ruptured pollen a high gain photodetector will be required. The most suitable commercially available detectors are photomultiplier tubes (PMT) and silicon photomultipliers (SiPM). Photomultiplier tubes consist of a glass (or similar transparent material) envelope, a photocathode, and a series of dynodes. Photomultiplier tubes operate when an incident photon/s hit the photocathode resulting in an emitted electron/s that are accelerated and amplified by the dynodes which can result in gains exceeding 10^6 (Hamamatsu 2007). Photomultiplier tubes require a high voltage supply ($> 1000V$) to drive the dynodes and are susceptible to damage from intense light sources when energised.

Silicone photomultipliers are semiconductor devices that consist of an array of single pho-

ton avalanche photodiodes. SiPM operate where the reverse bias voltage across the p-n junction exceeds the breakdown voltage of the junction resulting in a very high electric field across the device (SensL 2018). When a photon strikes the device an avalanche of electrons are displaced causing a sharp rise in current. When this occurs the integrated quenching resistor, lowers the reverse bias voltage across the junction quenching the avalanche and resetting the diode (SensL 2018). Depending on the reverse bias voltage, gain can approach 10^6 . Silicon photomultipliers operate with low reverse bias voltages ($< 30V$) and are not damaged by high intensity incidental light.

For this design, the SiPM has been chosen as the detector because of low biasing voltages and not being susceptible to damage by high intensity incidental lighting.

Optics The primary optical component of the prototype sensor is the bandpass filter for the detector. A filter with a centre wavelength of $340\text{ nm} \pm 10\text{ nm}$ is the preferred option to limit interference from unwanted sources.

3.5 Chapter Summary

Critical evaluation of the literature review has indicated that ultraviolet light induced protein fluorescence should be the most suitable detection technique for the development of the sensor system. Analysis of the chemical and physical characteristics of pollen suggests that targeting the fluorescent amino acids tryptophan and tyrosine should provide a suitable means to detect airborne biological particles. This approach could also aid in the discrimination between organic and inorganic particles as inorganic particles would not contain amino acids. For the prototype design the sensor system will utilise an 280 nm UV LED for the light source, a 340 nm \pm 10 nm UV bandpass filter, and a SiPM as the photodetector.

Chapter 4

System Design and Experimental Verification of Concepts

4.1 Chapter Overview

The purpose of this chapter is to outline the development process for the pollen sensing system. This section will deal primarily with the theoretical design, practical implementation, and experimental verification of the validity of using intrinsic protein fluorescence for the detection of pollen particles.

To develop the sensor system an understanding of the signal level obtained from the irradiated pollen is essential to be able to design the necessary amplifiers and data acquisition circuitry. To acquire this knowledge several graded experiments were undertaken using tryptophan and pollen.

4.2 System Design

4.2.1 Component Selection

The selection of components for the project was based on performance, cost, and availability of the necessary materials from major electronic suppliers. Due to the impact of COVID-19 and the shutting of borders in early 2020 the components that were selected

for this design were adequate (not necessarily optimal) and available for a reasonable price.

Ultraviolet Light Emitting Diode The UV LED that was selected for this design was the RayVio RVXD-280-SB-071005. The LED has a 280 nm nominal wavelength with 4 mW of radiant power in a star board package and costs \$28 AUD. The spectra of the LED's output is shown in figure 4.1 and should be suitable for the design.

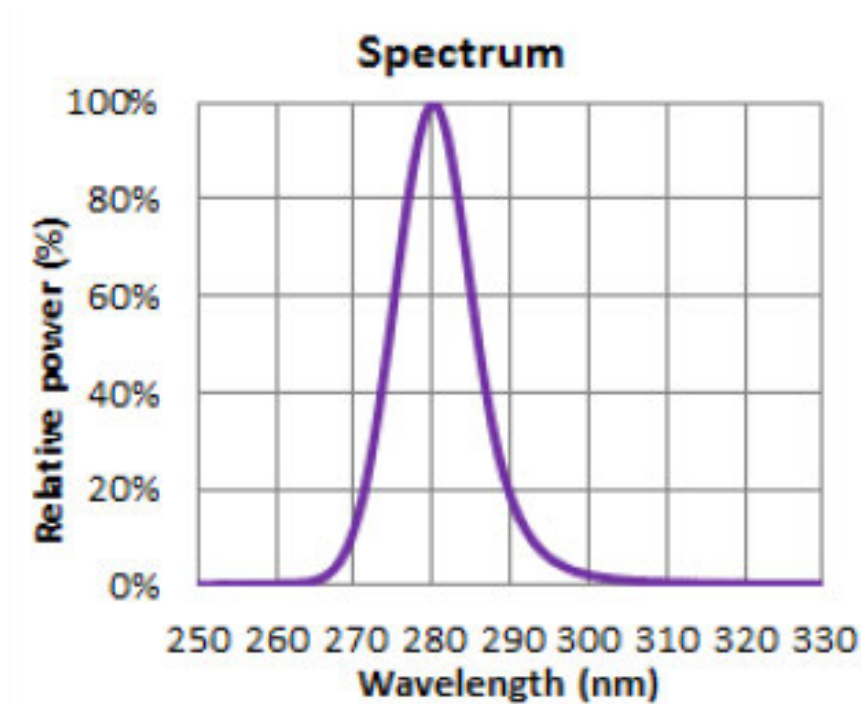


Figure 4.1: Spectrum of the RVXD-280-SB-071005 (RayVio 2020).

Silicon Photomultiplier The silicon photomultiplier chosen for the design was the SensL MICROFC-SMTPA-60035-GEVBOS-ND. The SiPM is a 6 mm² sensor with 35 μ m microcells packages on a development board for ease of prototyping and costs \$158 AUD. The spectral range of the SiPM is 300 nm to 950 nm with a photon detection efficiency of approximately 22% at 340 nm as shown in figure 4.2.

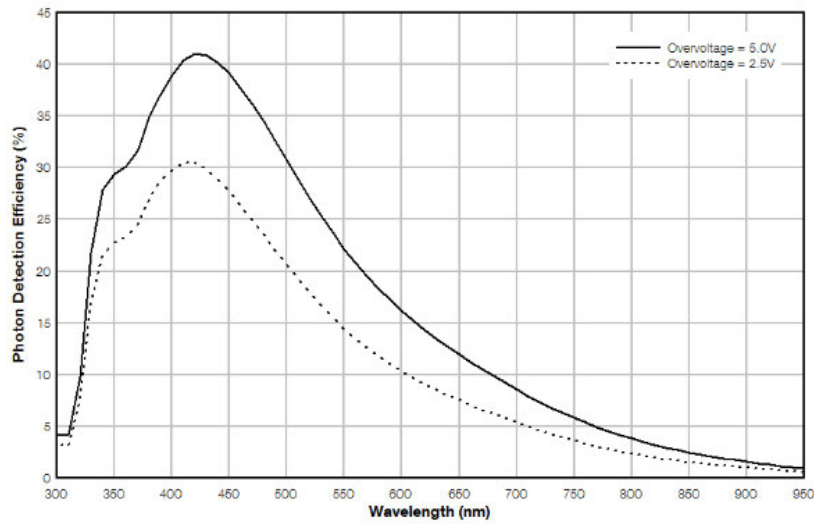


Figure 3. PDE versus Wavelength

Figure 4.2: SiPM PDE versus Wavelength (Lakowicz 2007).

Optical Filter The optical bandpass filter for the design was sourced from Thorlabs and is the FB340-10 with a 24.5 mm external diameter and a centre wavelength of $340 \text{ nm} \pm 2 \text{ nm}$ with a full width at half maximum of $10 \text{ nm} \pm 2 \text{ nm}$ as shown by figure 4.3. The Thorlabs filter was chosen for this design based on availability and cost approximately \$200 AUD.

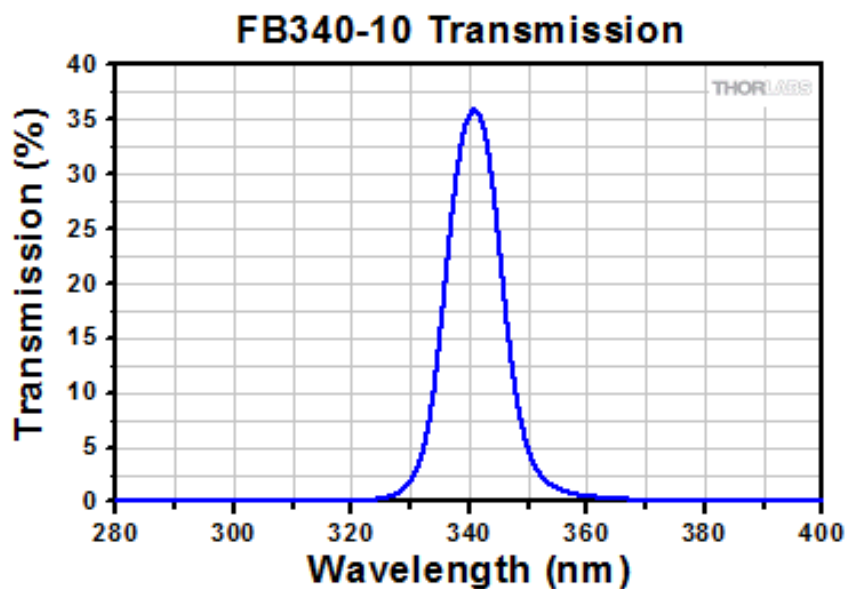


Figure 4.3: Optical Bandpass Filter Transmission (ThorLabs 2020).

4.3 Initial Testing of the Silicon Photomultiplier

To determine operational requirement and the intrinsic characteristics of the SiPM a series of preliminary experiments were conducted to verify the operation of the circuitry. The first test was to confirm that the SiPM was functioning correctly by measuring the flicker of fluorescent lighting with the second test to measure the dark current of the sensor to compare against the values stated in the data sheet.

Test Circuit Initial testing of the SiPM was conducted using the recommended circuit from the datasheet which utilises a current sensing resistor to measure the current draw of the SiPM. The sensor was positively biased at 27 V with the power supply rails being filtered using the recommended generic filter arrangement. The test circuit was constructed on a solderless breadboard.

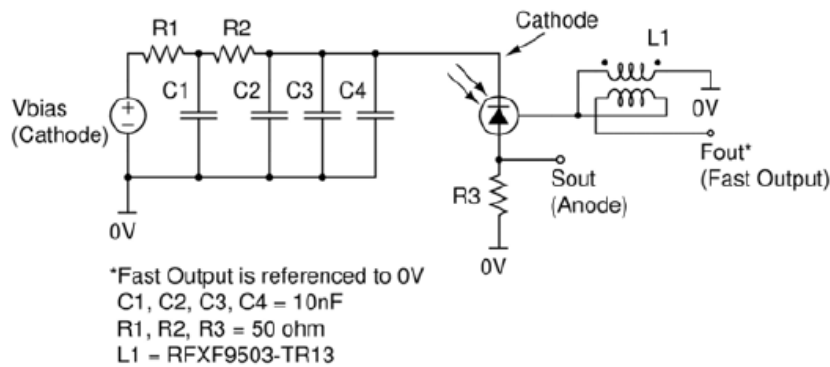


Figure 4.4: SiPM test circuit showing filter and current sensing resistor.

4.3.1 Fluorescent Light Flicker

The goal of this test was to verify the correct operation of the SiPM and associated circuitry. This was done by using the SiPM to measure the 100 Hz flicker present in fluorescent lighting. The SiPM was biased with 27 V and the output of the sensor connected to an oscilloscope for measurement.

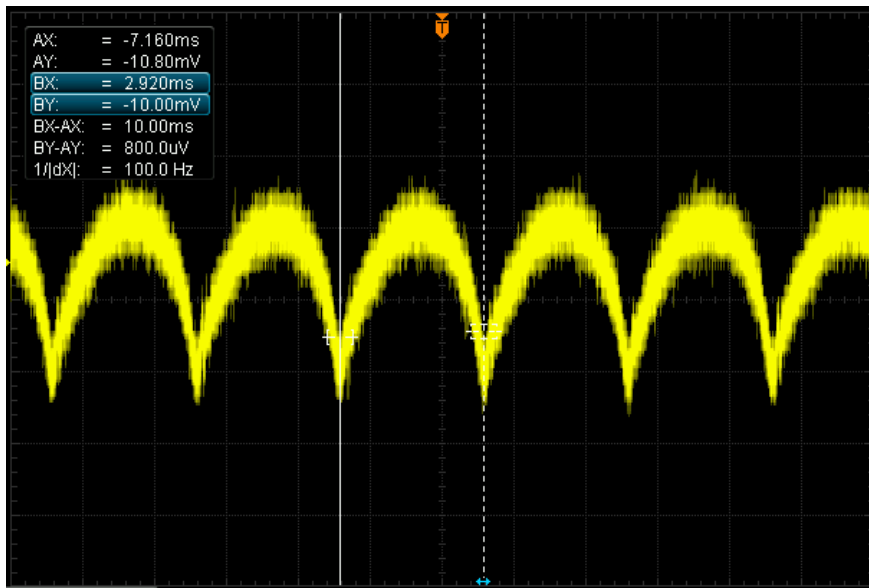


Figure 4.5: Fluorescent light flicker trace.

Analysis of the trace in figure 4.5 shows that the frequency of the flicker is approximately 100 Hz. This is consistent with a 50 Hz mains supply as the fluorescent lighting emits photons at the peaks and troughs of the alternating current (AC) mains cycle. This indicates that the SiPM and associated circuitry was working as expected.

4.3.2 Dark Current Measurement

The dark current of the SiPM is the noise generated by the device when there is no incidental light falling on the photosensitive area of the SiPM. The dark current was measured from the SiPM to verify correct operation as per the datasheet and to provide a starting point for experimentations. For this experiment the SiPM was biased with 27 V and was conducted in the dark box to exclude the influence of incidental light.

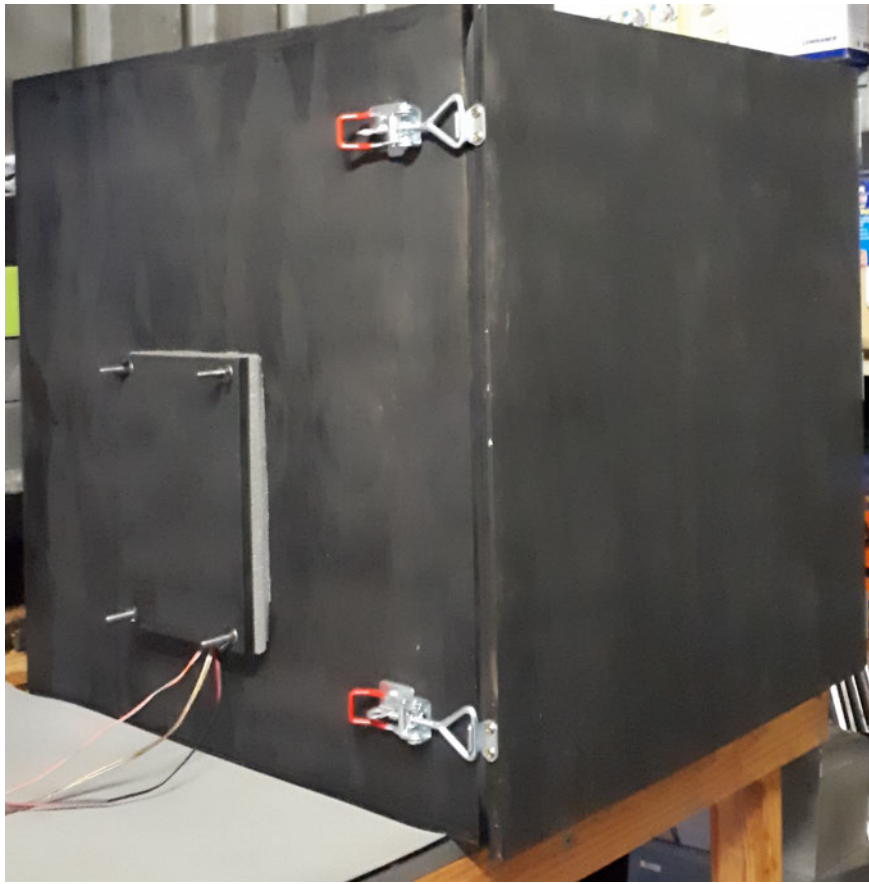


Figure 4.6: Dark Box.

The measured dark current for the SiPM had an average of approximately 600 nA which is below the datasheet specification of 618 nA typical.

4.4 Verification of Tryptophan Fluorescence

With verification that the SiPM and associated circuitry is functioning within specified parameters the next experiment to be perform is to confirm the fluorescent properties of tryptophan. For this experiment tryptophan was acquired as a dietary supplement from SuperiorLabs. The supplement is supplied in capsule form with each capsule containing 500 mg of L-Tryptophan and organic rice concentrate. Weight measurement of a capsules contents reveals that 160 mg of organic rice concentrate is present in each capsule representing approximately 24% of the contents.

To establish that UV fluorescence of tryptophan is a viable detection method for proteins (using limited resources) a simple proof of concept experiment was devised. The aim was

to determine if the photomultiplier and bandpass filter assembly could be used to detect the fluorescence of tryptophan from a UV LED. The assembly was built onto a solderless breadboard and with the SiPM biased with 27 V and the UV LED driven with 30 mA. With the apparatus set up the photomultiplier was powered on and a background reading was established figure 4.7. Next a glass slide with tryptophan was placed near the sensor and illuminated with UV light from the LED to fluoresce figure 4.8. The reading on the connected multimeter went from 0.173 mV to 1.521 mV indicating a positive detection. A blank slide (without tryptophan) was placed in the same position with the reading only increasing to 0.25 mV.

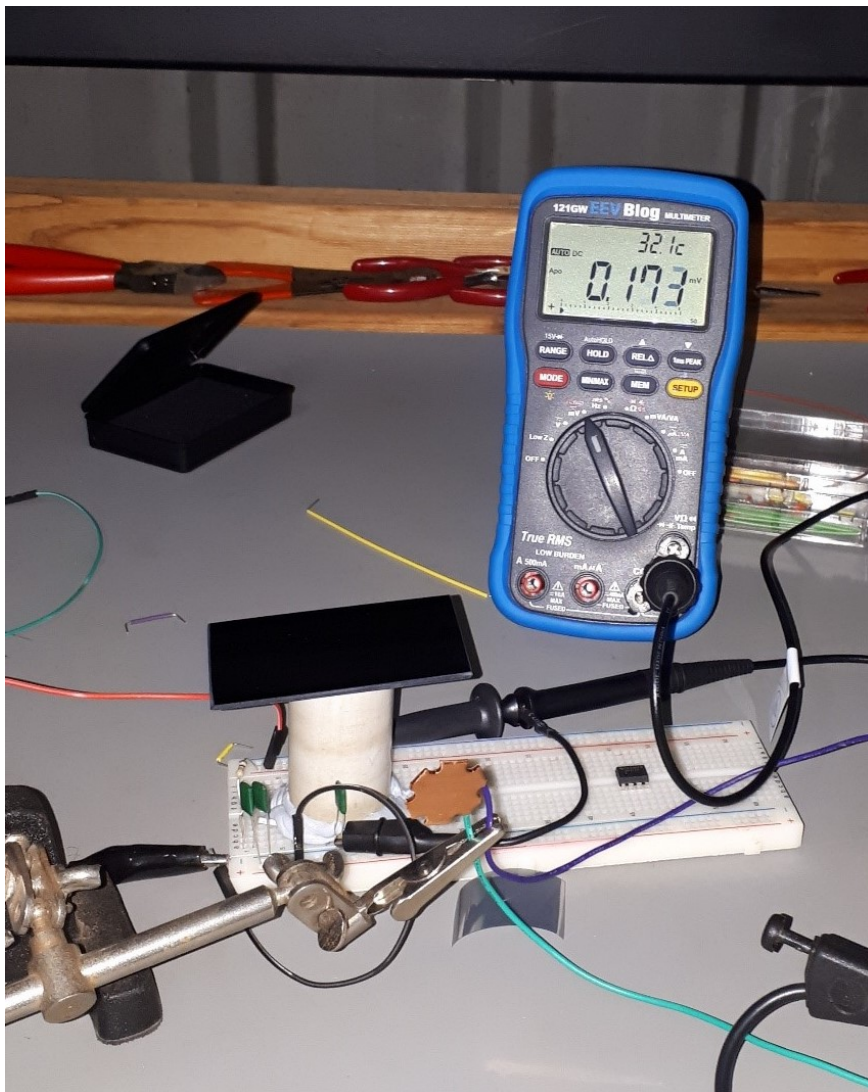


Figure 4.7: SiPM ambient light reading.

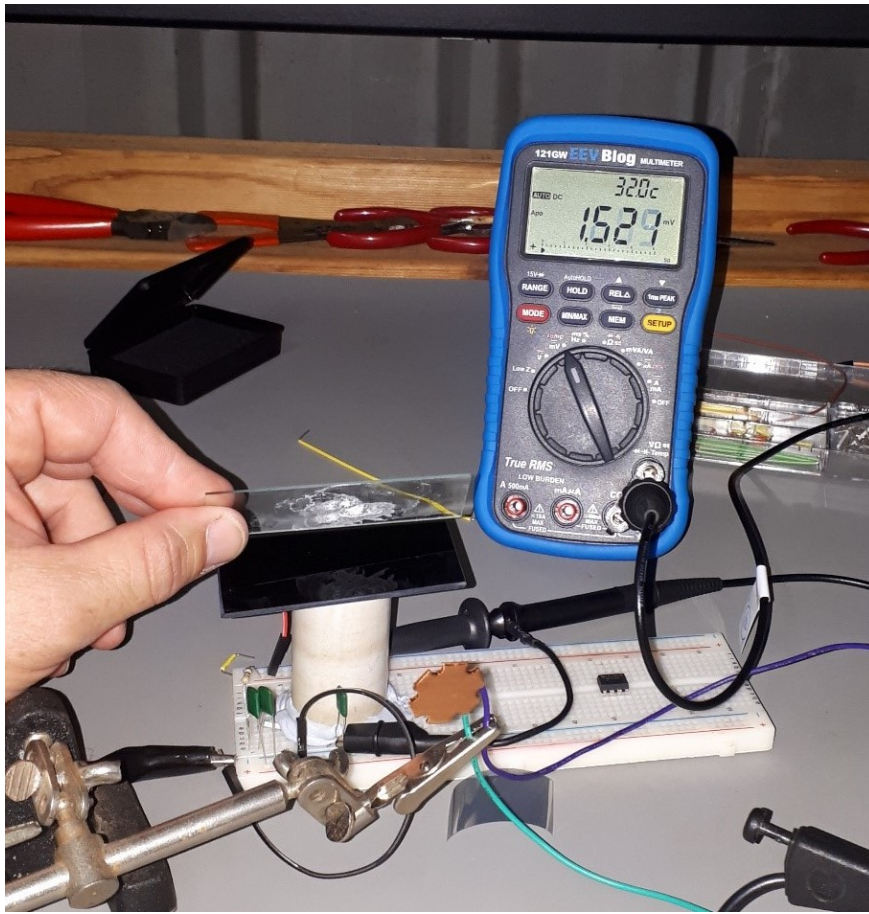


Figure 4.8: Tryptophan fluorescence.

4.5 Pollen

The pollen used for this series of experiments was obtained primarily from a hibiscus plant figure 4.9. This choice was made due to the high availability of samples (consistent flowering of the plant) and the size of the hibiscus pollen grains $20\text{--}80\ \mu\text{m}$ (measured) which made preparing samples easier figure 4.10.



Figure 4.9: Hibiscus flower.

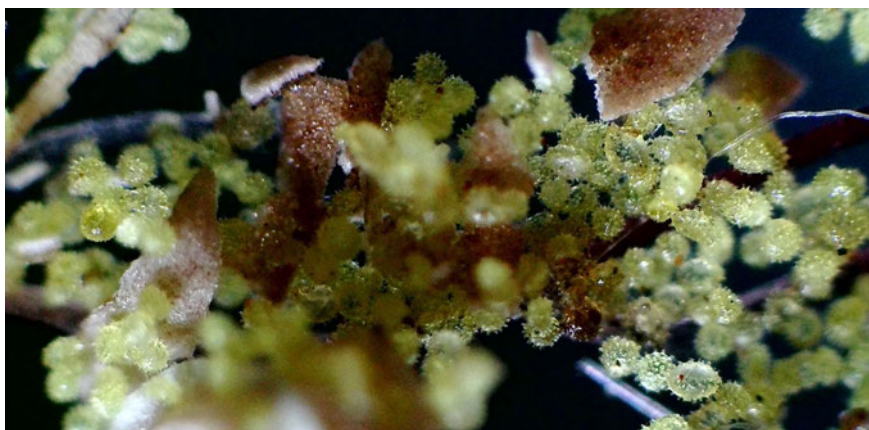


Figure 4.10: Hibiscus pollen.

4.6 Phase 1: Fluorescence of Multiple Pollen Grains

The first phase of testing with pollen is to determine if it is possible to detect the fluorescence of the pollen grains with multiple grains being irradiated simultaneously. The reasoning is that with an increased amount of pollen present the fluorescent emissions will be greater and easier to detect. This experiment should provide information about the sensitivity of the system.

Test Circuit The test circuit was constructed onto stripboard and utilises the generic power supply filter as per the datasheet with the addition of a $1\text{ M}\Omega$ current sensing resistor. The prototype circuit board was assembled into a 3D printed enclosure with the optical bandpass filter installed. The SiPM is biased at 27 V with the UV LED driven with 30 mA at approximately 1 mW radiant output.

Experimental Setup The experiment test jig was assembled and placed into the dark box to minimize stray light interference to obtain more consistent results. The sensor was mounted directly above the sample slide with the UV LED at right angles to the sample slide to minimise reflection of the UV light into the sensor viewing window figure 4.11.

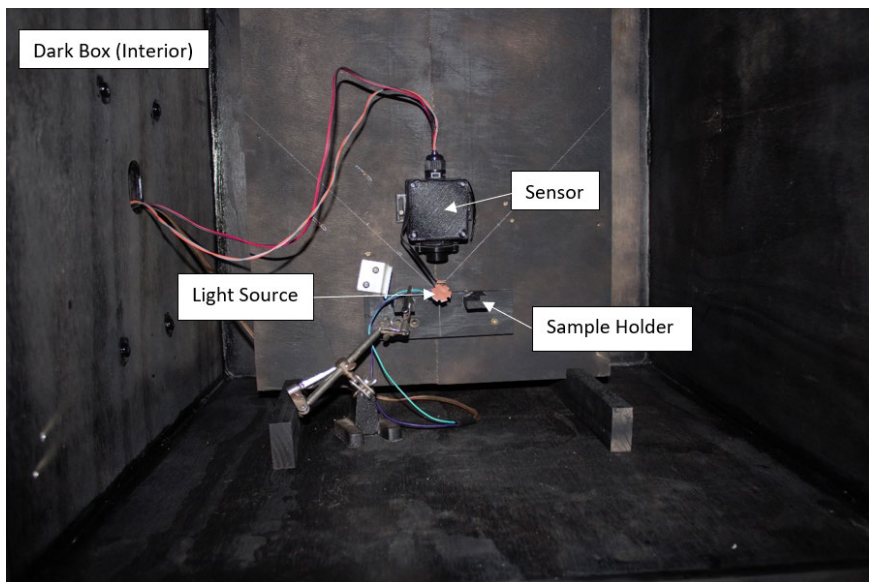


Figure 4.11: Setup of sample holder.

Samples Two pollen samples were prepared and placed onto two clean blank slides figure 4.12. The prepared slides were then stored in the dark box (clean and dust free environment) ready for use.



Figure 4.12: Hibiscus pollen sample.

Experimental Procedure The experiment will test the two prepared pollen samples and use two blank slides as controls to test for the detection of fluorescence. The first run involved taking a reading from a blank slide (1) and noting the average reading after 10 seconds of exposure. Then a slide with a pollen sample (1) was placed in the holder and irradiated for 10 seconds with the average reading taken. This procedure was repeated for the other pollen sample (2) and blank slide (2). When the first run was completed 3 more subsequent runs were undertaken with the result recorded in table 4.1.

Table 4.1: Voltage readings from irradiated pollen for each run.

Run/Sample	Blank 1	Sample 1	Blank 2	Sample 2
Run 1	1010 mV	1018 mV	980 mV	988 mV
Run 2	995 mV	1001 mV	992 mV	995 mV
Run 3	989 mV	988 mV	985 mV	990 mV
Run 4	990 mV	982 mV	978 mV	989 mV

Analysis The purpose of retesting the samples multiple times was to verify that the results were correct and not caused by random noise and other influencing factors. From

the initial series of results, it would seem that the first run did indeed indicate that fluorescence was occurring, and that detection was established. Interestingly, subsequent runs did not show the same results as run 1. Further testing using the same procedure produced similar results to the first series of trials and suggests that intrinsic protein fluorescence is not a suitable sensing method for pollen.

Explanation After considering the results and doing more experimentation and research a possible explanation was discovered. Photobleaching may be occurring which is resulting in the pollen grains fading. The UV light source causes photon-induced damage to the fluorophore molecules. When the molecules are in an excited state the molecules can interact with surrounding chemical compounds which causes irreversible covalent modification resulting in the molecule no longer fluorescing (Nikon 2020) . This problem may have been compounded by storing the test samples in the dark box while the UV LED was energised.

4.7 Phase 2: Verification of Photobleaching

This experiment was designed to ascertain if photobleaching of the fluorophores in the pollen samples was resulting in unstable readings.

Test Circuit The test circuit was constructed onto stripboard and utilises the generic power supply filter as per the datasheet with the current draw of the sensor being directly measured by a multimeter. The prototype circuit board was assembled into a 3D printed enclosure with the optical bandpass filter installed. The SiPM is biased at 27 V with the UV LED driven with 30 mA at approximately 1 mW radiant output.

Experimental Setup The experiments were conducted in a ‘dark box’ to minimise stray light interference, dust and to prevent exposure to UV light. The sensor is positioned directly above the sample to be tested with the light source being approximately 90° to the sensor to minimise reflections. The sample sits on the sample holder and positions the slide under the sensor as shown in figure 4.11. The measuring device and power supply are outside of the dark box.

Experimental Procedure To test this hypothesis a series of tests were performed using the sensor with and without fluorophores present in the test chamber for a nominal period

of 180 seconds. The first test is to measure the dark current and establish a baseline for the sensors noise levels. The second test was to measure the photobleaching of a sample of tryptophan and track the decrease in brightness over time to establish if photobleaching was indeed evident. The third test was divided into 3 groups with group 1 measuring the fluorescent intensity of freshly prepared samples of pollen (new), group 2 measuring the fluorescent intensity of previously irradiated pollen samples (old), and group 3 measuring the system performance without pollen samples present (blank slides) to determine if the decrease measured fluorescent intensity is due to other system factors, such as a decreasing output or a frequency shift from the UV LED as the die temperature increases during use. The intensity of the emitted light is determined by measuring the current draw of the SiPM using a logging multimeter.

Results The logged current values for all the experiments are shown in the following figures. Figure 4.13 shows the measured quiescent current draw of the SiPM under no light conditions and is within specification as stated in the datasheet with a variation of about 30 nA. Figure 4.14 was the test involving the tryptophan sample and clearly shows a decrease in intensity of the fluorescent emissions as the sample is irradiated over time and suggests photobleaching maybe occurring. The next series of results figure 4.15 displays the test results of the sensor system when blank slides were placed in the holder and does show a decrease of measured intensity over the course of the experiment. This could be caused by fluorophores present in the test chamber, surface contamination of the blank slides or reduction of light intensity from the UV light source as it heats up. Figure 4.16 displays the results of the measurements of the intensity of the fluorescent emissions of the pollen sample both new and previously irradiated. The samples that have been irradiated in past experiments exhibited characteristics like the blank slides. The new samples of pollen display strong initial emissions but quickly degrade over the course of the tests. This is consistent with the results obtained by the tryptophan and suggest the photobleaching is occurring with the pollen samples.

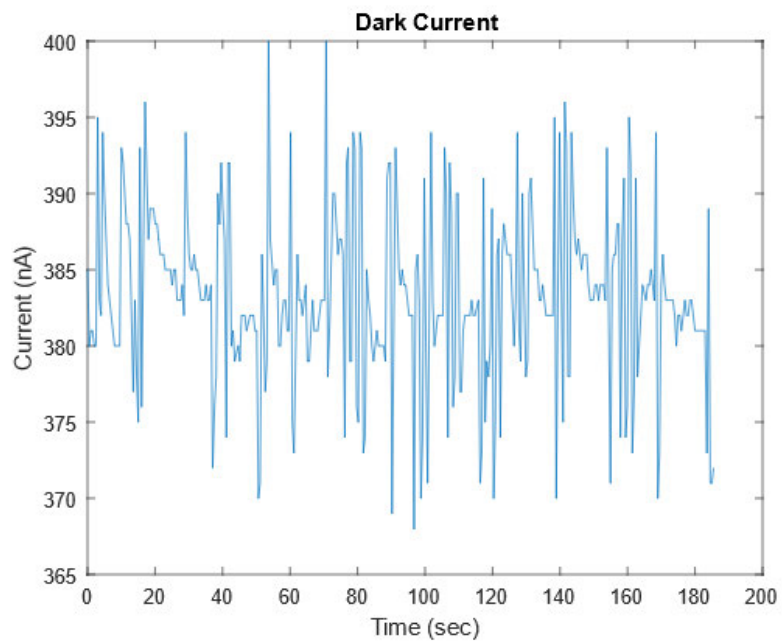


Figure 4.13: Dark current measurements.

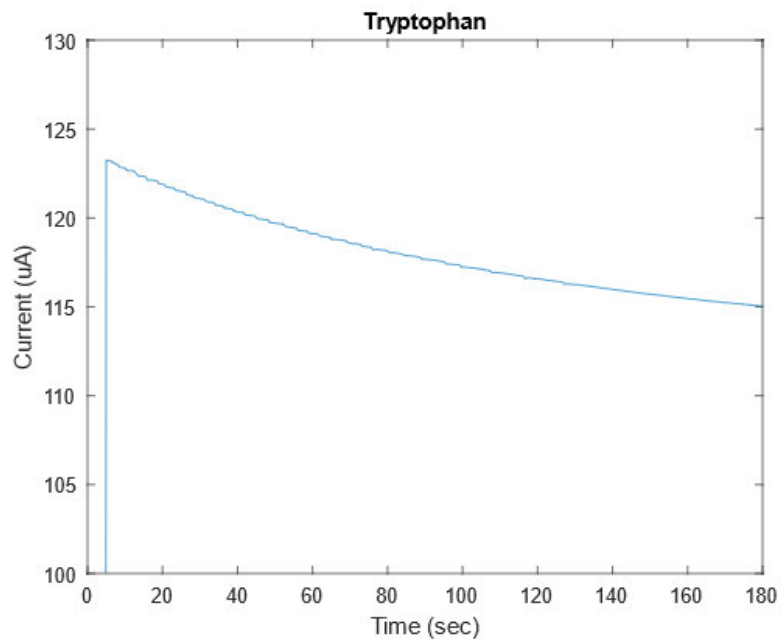


Figure 4.14: Intensity of tryptophan sample with continuous irradiation.

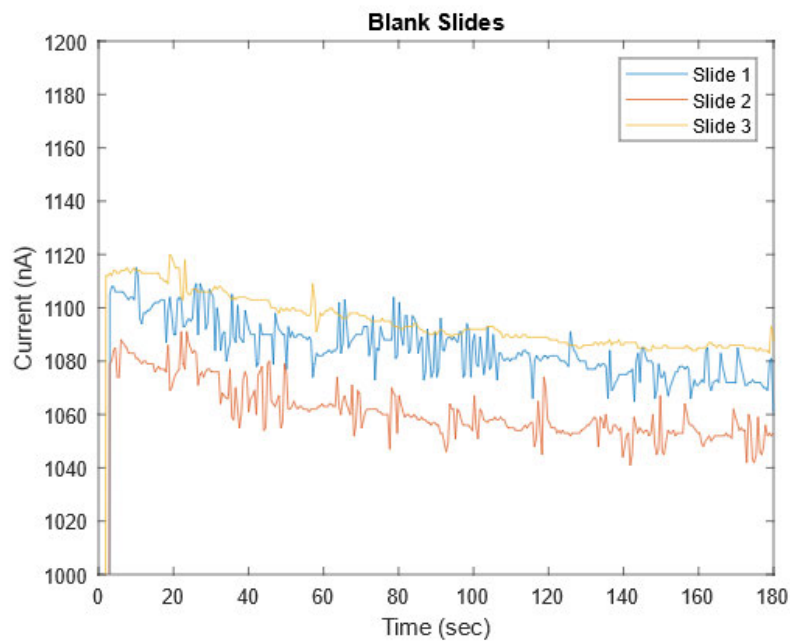


Figure 4.15: Continuous irradiation of blank slides.

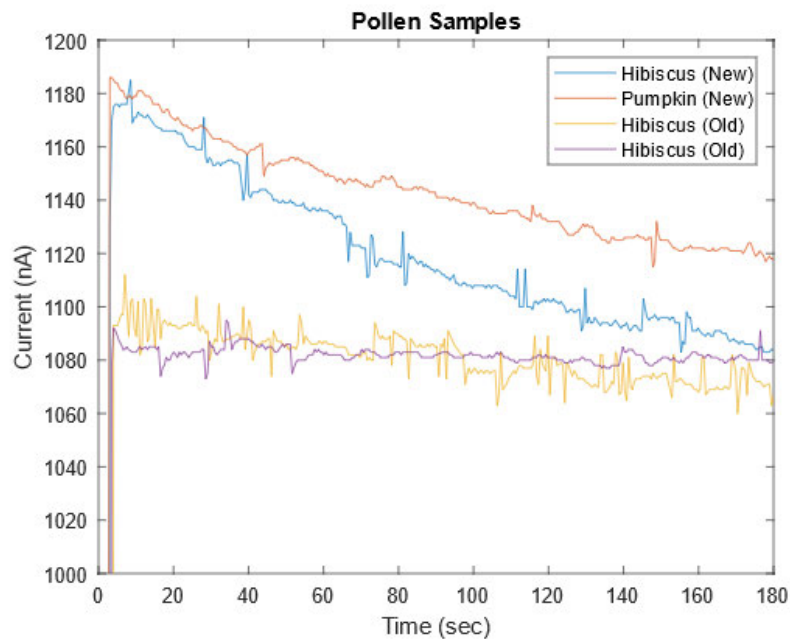


Figure 4.16: Photobleaching of pollen samples.

Analysis The photobleaching of the samples provides strong evidence that the measured emissions are from fluorescence and not reflections. As the new samples of pollen have a strong initial response to the light source and have a clear decrease in fluorescent intensity the longer the samples are irradiated suggests photobleaching. The old samples that have been exposed to the UV light source before do not demonstrate the same strong ini-

tial response or the decrease in emissions suggesting the fluorophores have already been photobleached. If the measured emissions from the samples were due to reflection or scattering, then the measured intensity would not decrease over time and would remain reasonably constant. The results from this experiment provide insight into the intricacies of the sensor system and demonstrates that intrinsic protein fluorescence is a viable method of detecting pollen.

4.8 Phase 3: Fluorescence of a Single Pollen Grain

The purpose of this experiment is to verify if a single grain of pollen can be detected via fluorescence emissions using the SiPM based sensor system.

Test Circuit Remains the same as the previous set of experiments with the SiPM being biased at 27 V and the UV LED driven with 80 mA at approximately 3.2 mW radiant output.

Experimental Setup The experiments were conducted in a ‘dark box’ to minimise stray light interference, dust and to prevent exposure to UV light. The sensor is positioned directly above the sample to be tested with the light source being approximately 90° to the sensor to minimise reflections. The sample sits on the sample holder which positions the slides under the sensor figure 4.11. The measuring device and power supply are outside of the dark box.

Experimental Procedure For this experiment the detection of fluorescence will rely upon measuring the effect of photobleaching on the pollen sample. To mitigate any possible effect that heating of the LED may have on changing the output intensity of the LED an aluminium heatsink (thermal mass) was added to the system. The LED was temperature stabilise for 5hrs before any experiments were undertaken. With the temperature stabilisation complete a blank slide was placed in the holder and measurements taken over a 180 seconds period. Next the pollen sample was placed in the holder and irradiated for 180 seconds with measurements taken. Finally, another blank slide was exposed for 180 seconds with readings taken.

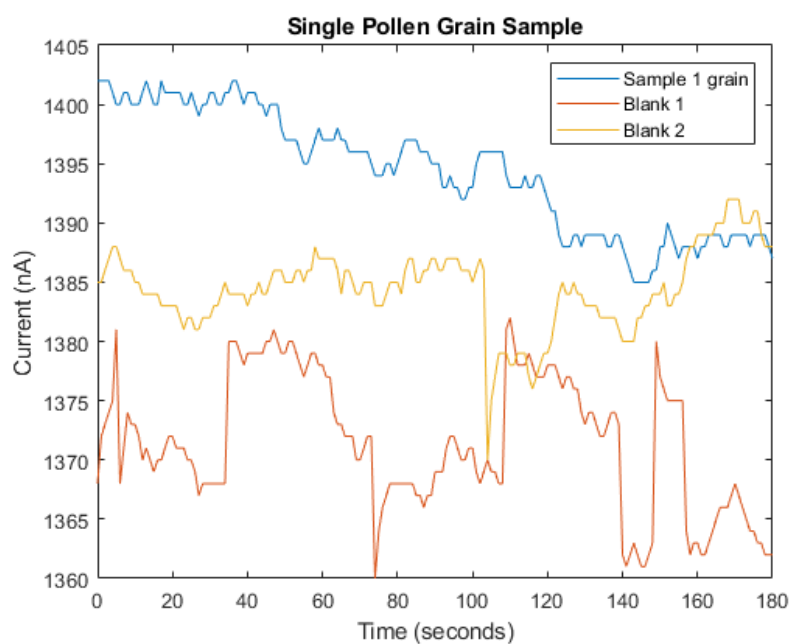


Figure 4.17: Trace showing photobleaching of a single pollen grain.

Analysis of the results in figure 4.17 show the characteristic decay of intensity consistent with photobleaching. This is a strong indicator that measurement of the fluorescence of a single pollen grain has been achieved. This result confirms that UV light induced fluorescence is a viable method for single particle detection of airborne pollen.

4.9 Chapter Summary

A series of graded experiments were undertaken to verify the correct operation of the silicon photomultiplier, associated circuitry, and to determine if protein fluorescence was a viable method for the detection of pollen. With the correct operation of the SiPM verified, several experiments were performed to measure the fluorescent emissions of multiple pollen grains (20-30) with the results clearly showing a distinctive decrease in brightness from the sample under continuous irradiation. This decrease in brightness was also measured from a sample using a single grain of hibiscus pollen. This suggests that photobleaching of the fluorophores is occurring indicating the emissions being measured are from ultraviolet light induced fluorescence of the pollen amino acids.

Chapter 5

Conclusions and Further Work

5.1 Conclusions

The purpose of this study was to provide the foundation knowledge and design elements to develop a deployable cost-effective real-time pollen detection system. The primary goal of this project was to develop the sensor using cost-effective materials and components that are readily available from major electronics supply companies. The system is intended to provide real-time bioaerosol particle counts and provide a timely warning of abnormal situation that could precede a thunderstorm asthma epidemic as was experience by Melbourne on the 21st of November 2016. To achieve this goal, a literature review was undertaken to determine the current state of development of bioaerosol sensing techniques and systems and to establish the physical and chemical properties of pollen. Evaluation of the chemical and physical characteristics of pollen suggests that targeting the fluorescent aromatic amino acids tryptophan and tyrosine should provide a suitable means to detect airborne biological particles. From these findings fluorescent spectroscopy was ascertained to be the best candidate for development of the sensor. A prototype fluorescent sensor was built using a 280 nm UV LED for the light source, a $340 \text{ nm} \pm 10 \text{ nm}$ UV bandpass filter, and a blue sensitive silicon photomultiplier as the photodetector. With a working prototype a series of experiments were conducted to test the validity of using ultraviolet light induced fluorescence to detect pollen. Fluorescent emissions from irradiated pollen were measured from samples containing multiple pollen grains (20-30) and a single pollen grain. These detections were verified by measuring the photobleaching of the fluorophores which produced a measurable exponential decrease in

intensity over a 180 second period of constant illumination with 280 nm ultraviolet light. This project has successfully demonstrated that intrinsic protein fluorescence is a viable method for the detection of airborne pollen particles and could be used as the basis for the develop of a deployable real-time pollen detection system. If this system could be realised, then it is reasonable to assume that advanced warning of potential thunderstorm asthma epidemics could be achieved resulting in a positive benefit to public health which could potentially save lives.

5.2 Further Work

With the proof of concept confirmed and detection of single particle verified, the next step in the design phase is to test the sensitivity of the system to a moving pollen particle similar to what would occur if pollen was drawn through the sensor by a fan assembly. A test assembly will need to be constructed and a means of introducing a single pollen grain into an airstream will need to be realised. To improve the response time of the SiPM a transimpedance amplifier circuit will need to be implemented with the proposed design in appendix C. If this testing proves to be successful than it should be possible to construct a functioning prototype of the sensor system that could be field tested alongside a working pollen trap to verify correct operation in a real-world situation.

References

- Beggs, P. J. (2017), ‘Allergen aerosol from pollen-nucleated precipitation: A novel thunderstorm asthma trigger’, *Atmospheric Environment* **152**, 455–457.
- Blank, R., Vinayaka, P. P., Tahir, M. W., Vellekoop, M. J. & Lang, W. (2015), Optical sensor system for the detection of mold: Concept for a fully automated sensor system for the detection of airborne fungal spores, *in* ‘2015 IEEE Sensors’, pp. 1–4.
- brgfx (2020), ‘Common Flower Parts’. viewed 30 September, https://www.freepik.com/free-vector/common-flower-parts_2938224.htm.
- Carminati, M., Pedalà, L., Bianchi, E., Nason, F., Dubini, G., Cortelezzi, L., Ferrari, G. & Sampietro, M. (2014), ‘Capacitive detection of micrometric airborne particulate matter for solid-state personal air quality monitors’, *Sensors and Actuators A: Physical* **219**, 80 – 87. , viewed 30 September 2020, <http://www.sciencedirect.com/science/article/pii/S0924424714003987>.
- D’Amato, G., Liccardi, G. & Frenguelli, G. (2007), ‘Thunderstorm-asthma and pollen allergy’, *Allergy* **62**(1), 11–16. , viewed 30 september, <https://onlinelibrary.wiley.com/doi/abs/10.1111/j.1398-9995.2006.01271.x>.
- Dictionary, C. (2020), *Instrumentation of Fluorescence Spectroscopy (spectrofluorometer) and process*, Chemistry Dictionary. viewed 30 September 2020, <https://chemistry-dictionary.yallascience.com/2013/09/instrumentation-of-fluorescence.html>.
- Eyde, R. H. (2020), ‘Flower’.
- Fröhlich-Nowoisky, J., Kampf, C. J., Weber, B., Huffman, J. A., Pöhlker, C., Andreae, M. O., Lang-Yona, N., Burrows, S. M., Gunthe, S. S., Elbert, W., Su, H., Hoor, P., Thines, E., Hoffmann, T., Després, V. R. & Pöschl, U. (2016), ‘Bioaerosols in the

- earth system: Climate, health, and ecosystem interactions’, *Atmospheric Research* **182**, 346 – 376. , viewed 30 September 2020, <http://www.sciencedirect.com/science/article/pii/S0169809516301995>.
- Guest, C. (2017), *The November 2016 Victorian epidemic thunderstorm asthma event: an assessment of the health impacts*, State of Victoria, Department of Health and Human Services,. , viewed 30 September 2020, <https://www.google.com/url?sa=t&rct=j&q=&esrc=s&source=web&cd=&ved=2ahUKEWjo1N2Cvs7rAhUSwzGhBmYAEIQFjACegQIAhAB&url=https%3A%2F%2Fwww2.health.vic.gov.au%2FApi%2Fdownloadmedia%2F%257B459A8B36-7C70-4C0E-861E-C648BBF4C818%257D&usg=A0vVaw2hL-Uw4KEZvY2P1Jxhh1B1>.
- Halbritter, H., Ulrich, S., Grímsson, F., Weber, M., Zetter, R., Hesse, M., Buchner, R., Svojtka, M. & Frosch-Radivo, A. (2018), *Illustrated Pollen Terminology*, Springer International Publishing.
- Hamamatsu (2007), *Photomultiplier Tubes*, 3rd edn, Hamamatsu. viewed 30 September 2020, https://www.hamamatsu.com/resources/pdf/etd/PMT_handbook_v3aE.pdf.
- Harun, N.-S., Lachapelle, P. & Douglass, J. (2019), ‘Thunderstorm-triggered asthma: what we know so far’, *Journal of asthma and allergy* **12**, 101–108. , viewed 30 September 2020, <https://pubmed.ncbi.nlm.nih.gov/31190900>.
- Hooijschuur, J. H. (2020), ‘Fluorescence spectrometry’. viewed 30 September 2020, <https://www.chromedia.org/chromedia?waxtrapp=mkqjtbEsHiemBpdmBlIEcCARB&subNav=cczbdbEsHiemBpdmBlIEcCARBP>.
- Jensen, W. A., Fisher, D. B. & Ashton, M. E. (1968), ‘Cotton embryogenesis: The pollen cytoplasm’, *Planta* **81**(2), 206–228. , viewed 30 September 2020, <https://doi.org/10.1007/BF00417450>.
- Kadaikar, A., Guinot, B., Trocan, M., Amiel, F., Conde-Cespedes, P., Oliver, G., Thibaudon, M., Sarda-Estève, R. & Baisnée, D. (2019), Automatic pollen grains counter, *in* ‘2019 3rd International Conference on Bio-engineering for Smart Technologies (BioSMART)’, pp. 1–4.
- Kaliszewski, M., Włodarski, M., Młyńczak, J., Leśkiewicz, M., Bombalska, A., Mularczyk-Oliwa, M., Kwaśny, M., Buliński, D. & Koczyński, K. (2016), ‘A new real-time

- bio-aerosol fluorescence detector based on semiconductor cw excitation uv laser', *Journal of Aerosol Science* **100**, 14 – 25. , viewed 30 September 2020, <http://www.sciencedirect.com/science/article/pii/S0021850216300593>.
- Kawashima, S., Clot, B., Fujita, T., Takahashi, Y. & Nakamura, K. (2007), 'An algorithm and a device for counting airborne pollen automatically using laser optics', *Atmospheric environment (1994)* **41**(36), 7987–7993.
- Kaya, G. K. (2018), 'Good risk assessment practice in hospitals (doctoral thesis)' . , viewed 30 September 2020, <https://doi.org/10.17863/CAM.20813>.
- Kaye, P. H., Stanley, W. R., Hirst, E., Foot, E., Baxter, K. L. & Barrington, S. J. (2005), 'Single particle multichannel bio-aerosol fluorescence sensor', *Opt. Express* **13**(10), 3583–3593. , viewed 30 September 2020, <http://www.opticsexpress.org/abstract.cfm?URI=oe-13-10-3583>.
- Kogelschatz, U. (2003), 'Dielectric-barrier discharges: Their history, discharge physics, and industrial applications', *Plasma Chemistry and Plasma Processing* **23**, 1–46.
- Lakowicz, J. (2007), *Principles of Fluorescence Spectroscopy*, Springer US. , viewed 30 September 2020, <https://books.google.com.au/books?id=-PSybuLNxcAC>.
- Lee, J., Kronborg, C., O'Hehir, R. E. & Hew, M. (2017), 'Who's at risk of thunderstorm asthma? the ryegrass pollen trifecta and lessons learnt from the melbourne thunderstorm epidemic', *Respiratory Medicine* **132**, 146 – 148. , viewed 30 September 2020, <http://www.sciencedirect.com/science/article/pii/S0954611117303517>.
- LILEK, N., GONZALES, A. P., BOŽIČ, J., BOROVSČAK, A. K. & BERTONCELJ, J. (2015), 'Chemical composition and content of free tryptophan in slovenian bee pollen', *Journal of Food and Nutrition Research* **54**, 323 – 333.
- Losappio, L., Heffler, E., Contento, F., Falco, A., Cannito, C. & Rolla, G. (2012), '218 thunderstorm-related asthma in patients sensitised to olea europaea pollen: Twenty emergency department visits for asthmatic symptoms in one single day', *The World Allergy Organization Journal* **5**, S89–S89.
- Nikon (2020), 'Fluorophore photobleaching literature references'. viewed 30 September 2020, <https://www.microscopyu.com/references/fluorophore-photobleaching>.

- Panowicz, R., Miedzińska, D., Palka, N. & Niezgoda, T. (2011), ‘The initial results of the spectroscopy non-destructive investigations of epoxy-glass composite structure’.
- Pappas, C. S., Tarantilis, P. A., Harizanis, P. C. & Polissiou, M. G. (2003), ‘New method for pollen identification by ft-ir spectroscopy’, *Appl. Spectrosc.* **57**(1), 23–27. , viewed 30 September 2020, <http://as.osa.org/abstract.cfm?URI=as-57-1-23>.
- Quilichini, T. D., Grienenberger, E. & Douglas, C. J. (2015), ‘The biosynthesis, composition and assembly of the outer pollen wall: A tough case to crack’, *Phytochemistry* **113**, 170 – 182. , viewed 30 September 2020, <http://www.sciencedirect.com/science/article/pii/S0031942214001939>.
- RayVio (2020), ‘Xd series uv emitter or star board led (280 nm)’. viewed 30 September 2020, <http://www.rayvio.com/xdseries/>.
- SensL (2018), *Low Noise, Blue-Sensitive Silicon Photomultipliers*, SensL. ,viewed 30 September 2020, <https://sensl.com/downloads/ds/DS-MicroCseries.pdf>.
- Shimadzu (2020), *Particle Size Distribution Calculation Method*, Shimadzu. viewed 30 September 2020, <https://www.shimadzu.com/an/powder/support/practice/p01/lesson22.html>.
- Smith, B. C. (n.d.), *Fundamentals of Fourier transform infrared spectroscopy*, CRC Press, Boca Raton.
- Somerville, D. C. (2001), *Nutritional Value of Bee Collected Pollens*, NSW Agriculture. viewed 30 September 2020, http://www.nbba.ca/wp-content/uploads/2013/12/Nutritional_Value_of_Bee_Collected_Pollens.pdf.
- Sporomex (2020), *Spores and Pollens*, Sporomex. viewed 30 September 2020, <http://www.sporomex.co.uk/technology/51-pollenspores>.
- ThorLabs (2020), ‘Optical bandpass filter fb340-10’. viewed 30 September 2020, <https://www.thorlabs.com/thorproduct.cfm?partnumber=FB340-10>.
- Tobias, H. J., Schafer, M. P., Pitesky, M., Fergenson, D. P., Horn, J., Frank, M. & Gard, E. E. (2005), ‘Bioaerosol mass spectrometry for rapid detection of individual airborne mycobacterium tuberculosis h37ra particles’, *Applied and Environmental Microbiology* **71**(10), 6086–6095. , viewed 30 September 2020, <https://aem.asm.org/content/71/10/6086>.

- Šukienė, L., Šaulienė, I. & Bukantis, A. (2011), 'Evaluation of meteorological parameters influence upon pollen spread in the atmosphere', *Journal of Environmental Engineering and Landscape Management* **19**, 5–11.
- XenonFlashTubes.com (2020), *UV Quartz Flash Lamps*, XenonFlashTubes.com. viewed 30 September 2020, https://www.xenonflashtubes.com/uv-quartz-flash-lamps_16.

Appendix A

Project Specification

ENG 4111/2 Research Project

Project Specification

For: **Jonathon Straker**
Topic: Real-time Pollen Detection by Intrinsic Protein Fluorescence
Supervisors: Dr John Leis
Sponsorship: Faculty of Health, Engineering & Sciences
Project Aim: Develop a sensor and software system for the continuous real-time detection of pollen using Intrinsic Protein Fluorescence to identify Tryptophan.

Programme: Version 1, 17th March 2020:

1. Design and build a proof of concept test sensor and confirm detection of Tryptophan via Intrinsic Protein Fluorescence.
2. Build a test rig and experimentally determine the limits of detection on static particles.
3. Enhance the sensor systems and data collection devices to improve detection limits of $<10\mu\text{m}$ if needed.
4. Reconfigure the test rig for moving particles and experimentally determine the limits of detection.
5. If possible, optimise the sensor system for sub-micron particle detection.
6. Characterise the sensors performance in a laboratory setting and report.

As time and resources permit:

1. Research and build an aerosol generator to field test the sensor system.
2. Design a field test to test the sensors performance in a real-world setting using the aerosol generator and numerical modelling to predict detection rates.
3. Field test the sensor and report on findings comparing to model predictions.

Agreed:

Student Name: Jonathon Straker

Date: 18 March 2020

Supervisor Name: Dr John Leis

Date: 24 June 2020

Appendix B

Risk Assessment

B.1 Introduction

A comprehensive safety analysis of the major tasks associated with the project was undertaken using the risk assessment matrix in table B.1. The results of this risk assessment with the analysis of the risk, with and without control measures implemented is shown in table B.4.

B.2 Risk Assessment

Table B.1: Risk Matrix

Risk Matrix		Consequences				
		Negligible 1	Minor 2	Moderate 3	Major 4	Catastrophic 5
Likelihood	Almost Certain 5	Moderate 5	High 10	Extreme 15	Extreme 20	Extreme 25
	Likely 4	Moderate 4	High 8	High 12	Extreme 16	Extreme 20
	Possible 3	Low 3	Moderate 6	High 9	High 12	Extreme 15
	Unlikely 2	Low 2	Moderate 4	Moderate 6	High 8	High 10
	Rare 1	Low 1	Low 2	Low 3	Moderate 4	Moderate 5

(Adapted from Kaya 2018)

Table B.2: Description of consequences

Score	Name	Description
1	Negligible	Minimal injuries, no first aid required
2	Minor	Minor injuries, first aid may be required
3	Moderate	Moderate injuries, professional treatment will be required
4	Major	Major injuries/disability, professional treatment required
5	Catastrophic	Death or multiple permanent disabilities

(Adapted from Kaya 2018)

Table B.3: Description of likelihoods

Score	Name	Description
1	Rare	Will not occur for years
2	Unlikely	May occur but not expected to
3	Possible	Will occur but infrequently
4	Likely	Will occur regularly
5	Almost Certain	Will occur very soon

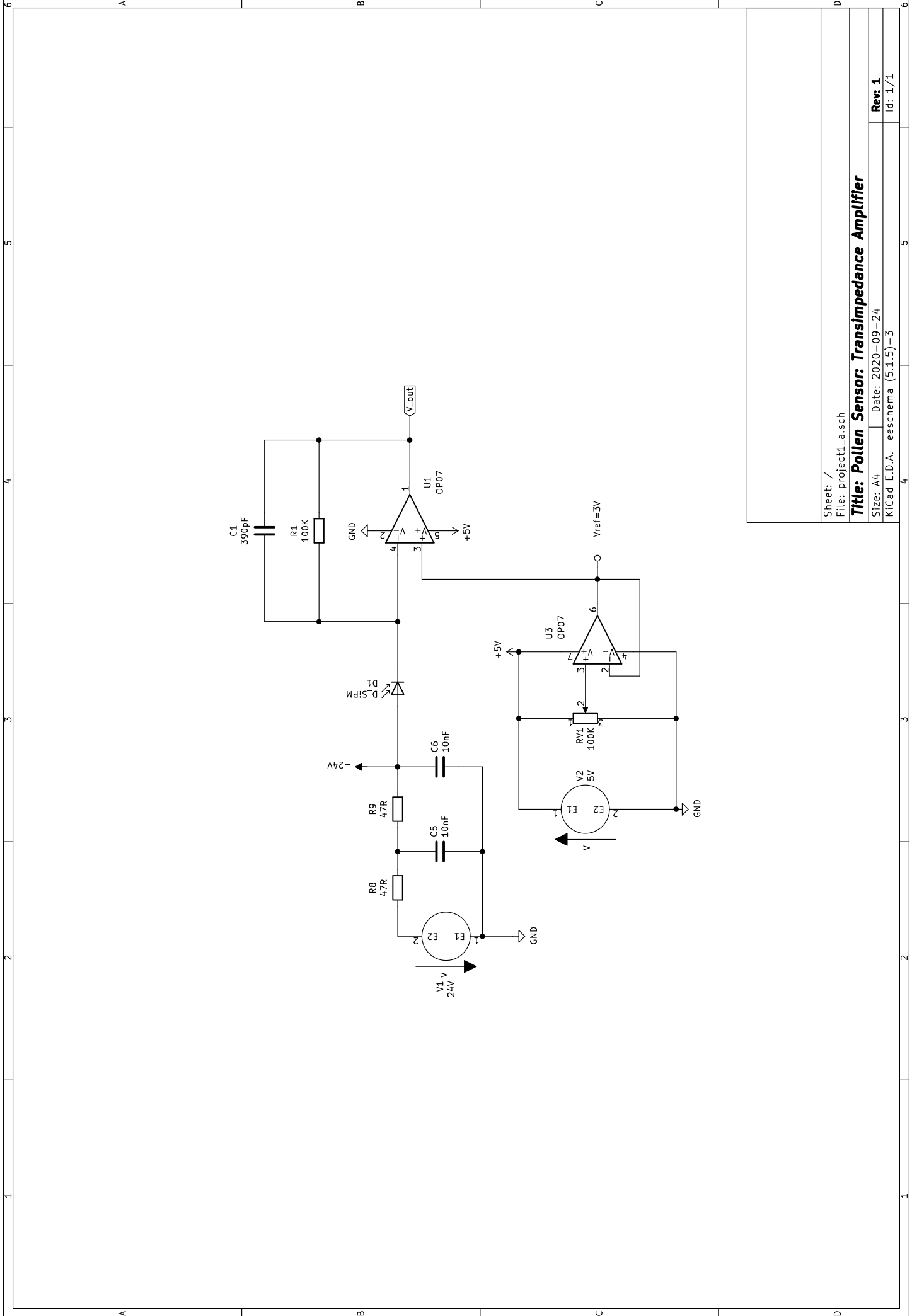
(Adapted from Kaya 2018)

Table B.4: Description of likelihoods

Activity or Equipment	Hazard	Consequences	Risk without controls	Controls	Risk with controls
Pollen Harvesting	Excessive sun exposure	Cancer, Burns	High 12	Sun protection	Low 3
Soldering	Hot surfaces	Burns	High 9	PPE	Low 2
Soldering	Solder fumes	Respiratory Irritation	High 9	Provide adequate ventilation	Low 2
UV Light Source	UV exposure	Burns, Eye damage	High 9	Light proof enclosure with interlock	Low 3
Using Hand Tools	Manual handling injuries to the body	Strains, sprains, cuts, bruises, etc.	High 12	PPE, proper use, and handling of equipment	Low 3
Glass Slides	Broken glass	Cuts	High 12	PPE, clean up broken glass promptly	Low 3

Appendix C

Schematic of Proposed Transimpedance Amplifier



Sheet: /
 File: project1_a.sch

Title: Pollen Sensor: Transimpedance Amplifier

Size: A4
 Date: 2020-09-24
 KiCad: E.D.A. eeschema (5.1.5)-3

Rev: 1
 Id: 1/1

Appendix D

Data Sheet: SensL C-Series SiPm

C-Series SiPM Sensors

Silicon Photomultipliers (SiPM), Low-Noise, Blue-Sensitive

The C-Series low-light sensors from ON Semiconductor feature an industry-leading low dark-count rate combined with a high PDE. For ultrafast timing applications, C-Series sensors have a fast output that can have a rise time of 300 ps and a pulse width of 600 ps. The C-Series is available in different sensor sizes (1 mm, 3 mm and 6 mm) and packaged in a 4-side tileable surface mount (SMT) package that is compatible with industry standard, lead-free, reflow soldering processes.

The C-Series Silicon Photomultipliers (SiPM) form a range of high gain, single-photon sensitive, UV-to-visible light sensors. They have performance characteristics similar to a conventional PMT, while benefiting from the practical advantages of solid-state technology: low operating voltage, excellent temperature stability, robustness, compactness, output uniformity, and low cost. For advice on the usage of these sensors please refer to the [Biasing and Readout](#) Application Note.



ON Semiconductor®

www.onsemi.com

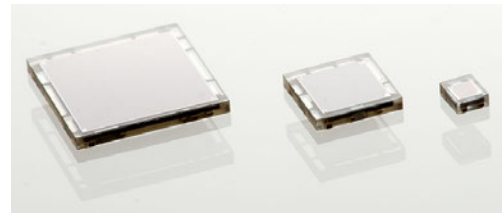


Figure 1. C-Series Sensors

ORDERING INFORMATION

See detailed ordering and shipping information on page 15 of this data sheet.

Table 1. PERFORMANCE PARAMETERS

Sensor Size	Microcell Size	Parameter (Note 1)	Overvoltage	Min.	Typ.	Max.	Units
1 mm	10μ, 20μ, 35μ	Breakdown Voltage (Vbr) (Note 3)		24.2		24.7	V
3 mm	20μ, 35μ, 50μ						
6 mm	35μ						
1 mm	10μ, 20μ, 35μ	Recommended overvoltage Range (Voltage above Vbr) (Note 2)		1.0		5.0	V
3 mm	20μ, 35μ, 50μ						
6 mm	35μ						
1 mm	10μ, 20μ, 35μ	Spectral Range (Note 4)		300		950	nm
3 mm	20μ, 35μ, 50μ						
6 mm	35μ						
1 mm	10μ, 20μ, 35μ	Peak Wavelength (λ _p)			420		nm
3 mm	20μ, 35μ, 50μ						
6 mm	35μ						

C-Series SiPM Sensors

Table 1. PERFORMANCE PARAMETERS (continued)

Sensor Size	Microcell Size	Parameter (Note 1)	Overvoltage	Min.	Typ.	Max.	Units								
1 mm	10 μ	PDE (Note 5) at λ_p	Vbr + 2.5 V	14			%								
	20 μ			24			%								
	35 μ			31			%								
1 mm	10 μ		PDE (Note 5) at λ_p	Vbr + 5.0 V	18			%							
	20 μ				31			%							
	35 μ				41			%							
3 mm	20 μ			PDE (Note 5) at λ_p	Vbr + 2.5 V	24			%						
	35 μ					31			%						
	50 μ					35			%						
3 mm	20 μ				PDE (Note 5) at λ_p	Vbr + 5.0 V	31			%					
	35 μ						41			%					
	50 μ						47			%					
6 mm	35 μ	PDE (Note 5) at λ_p				Vbr + 2.5 V	31			%					
6 mm	35 μ					Vbr + 5.0 V	41			%					
1 mm	10 μ					Gain (anode to cathode readout)	Vbr + 2.5 V	2×10^5							
	20 μ		1×10^6												
	35 μ		3×10^6												
3 mm	20 μ		Gain (anode to cathode readout)					Vbr + 2.5 V	1×10^6						
	35 μ			3×10^6											
	50 μ			6×10^6											
6 mm	35 μ			Gain (anode to cathode readout)					Vbr + 2.5 V	3×10^6					
1 mm	10 μ				Dark Current (Note 6)					Vbr + 2.5 V		1	3	nA	
	20 μ											5	16	nA	
	35 μ											15	49	nA	
3 mm	20 μ	Dark Current (Note 6)									Vbr + 2.5 V		50	142	nA
	35 μ												154	443	nA
	50 μ						319					914	nA		
6 mm	35 μ					Dark Current (Note 6)	Vbr + 2.5 V						618	1750	nA

C-Series SiPM Sensors

Table 1. PERFORMANCE PARAMETERS (continued)

Sensor Size	Microcell Size	Parameter (Note 1)	Overvoltage	Min.	Typ.	Max.	Units		
1 mm	10 μ	Dark Count Rate	Vbr + 2.5 V		30	96	kHz		
	20 μ				30	96	kHz		
	35 μ				30	96	kHz		
3 mm	20 μ				300	860	kHz		
	35 μ				300	860	kHz		
	50 μ				300	860	kHz		
6 mm	35 μ					1200	3400	kHz	
1 mm	10 μ , 20 μ , 35 μ			Rise Time – Fast Output (Note 7)		0.3		ns	
3 mm	20 μ , 35 μ , 50 μ					0.6		ns	
6 mm	35 μ		1.0		ns				
1 mm	10 μ , 20 μ , 35 μ	Signal Pulse Width – Fast Output (FWHM)		0.6		ns			
3 mm	20 μ , 35 μ , 50 μ			1.5		ns			
6 mm	35 μ			3.2		ns			
1 mm	10 μ	Microcell recharge time constant (Note 8)			5		ns		
	20 μ				23		ns		
	35 μ				82		ns		
3 mm	20 μ				23		ns		
	35 μ				82		ns		
	50 μ				159		ns		
6 mm	35 μ				95		ns		
1 mm	10 μ			Capacitance (Note 9) (anode–cathode)	Vbr + 2.5 V		50		pF
	20 μ						90		pF
	35 μ		100				pF		
3 mm	20 μ		770				pF		
	35 μ		850				pF		
	50 μ		920				pF		
6 mm	35 μ		3400				pF		
1 mm	10 μ	Capacitance (Note 9) (fast terminal to cathode)	Vbr + 2.5 V				1		pF
	20 μ						1		pF
	35 μ				1		pF		

C-Series SiPM Sensors

Table 1. PERFORMANCE PARAMETERS (continued)

Sensor Size	Microcell Size	Parameter (Note 1)	Overvoltage	Min.	Typ.	Max.	Units		
3 mm	20 μ	Capacitance (Note 9) (fast terminal to cathode)	Vbr + 2.5 V	20			pF		
	35 μ			12			pF		
	50 μ			7			pF		
6 mm	35 μ			48			pF		
1 mm	10 μ , 20 μ , 35 μ	Temperature dependence of Vbr		21.5			mV/°C		
3 mm	20 μ , 35 μ , 50 μ								
6 mm	35 μ								
1 mm	10 μ , 20 μ , 35 μ	Temperature dependence of Gain (Note 10)		-0.8			%/°C		
3 mm	20 μ , 35 μ , 50 μ								
6 mm	35 μ								
1 mm	10 μ	Crosstalk	Vbr + 2.5 V	0.6			%		
	20 μ			3			%		
	35 μ			7			%		
3 mm	20 μ			3			%		
	35 μ			7			%		
	50 μ			10			%		
6 mm	35 μ			7			%		
1 mm	10 μ			Afterpulsing	Vbr + 2.5 V	0.2			%
	20 μ					0.2			%
	35 μ	0.2					%		
3 mm	20 μ	0.2					%		
	35 μ	0.2					%		
	50 μ	0.6					%		
6 mm	35 μ	0.2					%		

1. All measurements made at 2.5 V overvoltage and 21°C unless otherwise stated.
2. Please consult the maximum current levels on page 6 when selecting the overvoltage to apply.
3. The breakdown voltage (Vbr) is defined as the value of the voltage intercept of a straight line fit to a plot of \sqrt{I} vs V, where I is the current and V is the bias voltage.
4. The range where PDE > 1% at Vbr + 5.0 V.
5. Note that the PDE does not contain contributions from afterpulsing or crosstalk.
6. Dark current derived from dark count data as $DC \times M \times q \times (1 + CT)$, where DC is dark count, M is gain, q is the charge of an electron, and CT is cross talk.
7. Measured as time to go from 10% to 90% of the peak amplitude.
8. RC charging time constant of the microcell (τ)
9. Internal capacitance of the sensor. Typically add 2–3 pF for sensor in package. Listed by unique microcell size for each part version.
10. Quoted as the percentage change per degree C from the measured value at 21°C.

C-Series SiPM Sensors

GENERAL PARAMETERS

Table 2. GENERAL PARAMETERS

	1 mm	3 mm	6 mm
	10010, 10020, 10035	30020, 30035, 30050	60035
Active area	1 × 1 mm ²	3 × 3 mm ²	6 × 6 mm ²
No. of microcells	10010: 2880 10020: 1296 10035: 504	30020: 10998 30035: 4774 30050: 2668	60035: 18980
Microcell fill factor	10010: 28% 10020: 48% 10035: 64%	30020: 48% 30035: 64% 30050: 72%	60035: 64%

Table 3. PACKAGE PARAMETERS

	1 mm	3 mm	6 mm
	10010, 10020, 10035	30020, 30035, 30050	60035
Package dimensions	1.5 × 1.8 mm ²	4 × 4 mm ²	7 × 7 mm ²
Recommended operating temperature range	-40°C to +85°C		
Maximum storage temperature	+105°C		
Soldering conditions	Lead-free, reflow soldering process compatible (MSL 3 for tape & reel quantities; MSL 4 for tape only qty.) See the SMT Handling Tech Note for more details.		
Encapsulant type	Clear transfer molding compound		
Encapsulant refractive Index	1.59 @ 420 nm		

Table 4. MAXIMUM CURRENT LEVELS FOR EACH SENSOR SIZE

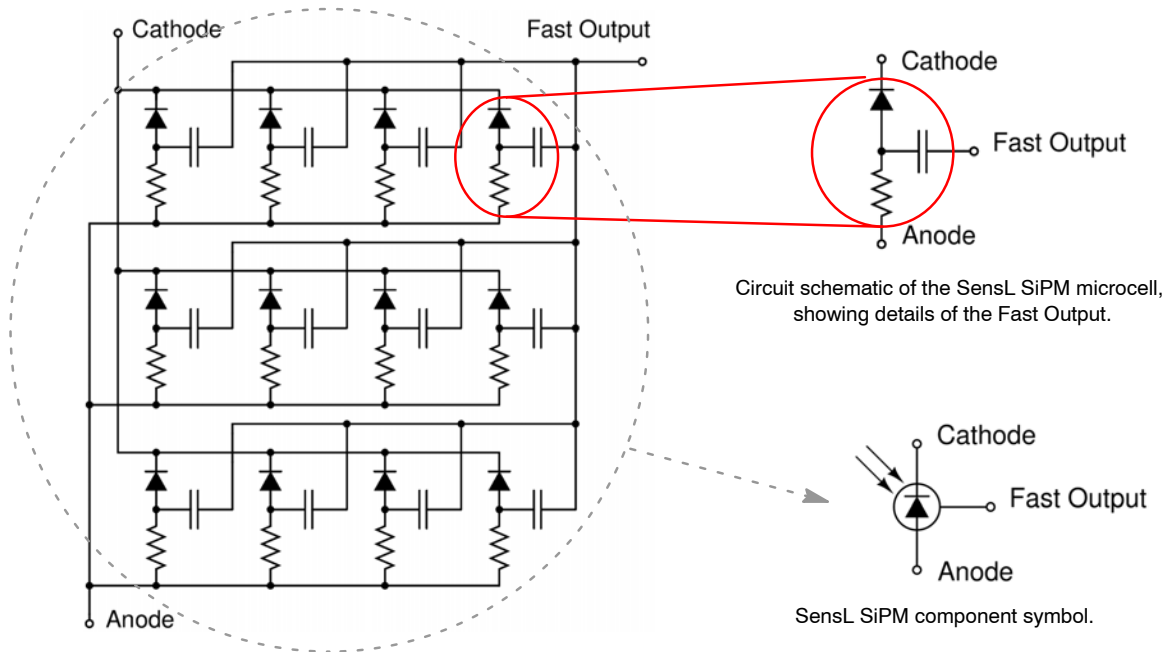
1 mm	3 mm	6 mm
10010, 10020, 10035	30020, 30035, 30050	60035
6 mA	15 mA	20 mA

C-Series SiPM Sensors

CIRCUIT SCHEMATICS

An SiPM is formed of a large number (hundreds or thousands) of microcells. Each microcell is an avalanche photodiode with its own quench resistor and a capacitively coupled fast output. These microcells are arranged in

a close-packed array with all of the like terminals (e.g. all of the anodes) summed together. The array of microcells can thus be considered as a single photodiode sensor with three terminals: anode, cathode and fast output.



Simplified circuit schematic of the SensL[®] SiPM showing only a 12 microcell example. Typically, SiPM sensors have hundreds or thousands of microcells.

Figure 2. Circuit Schematic

C-Series SiPM Sensors

PERFORMANCE

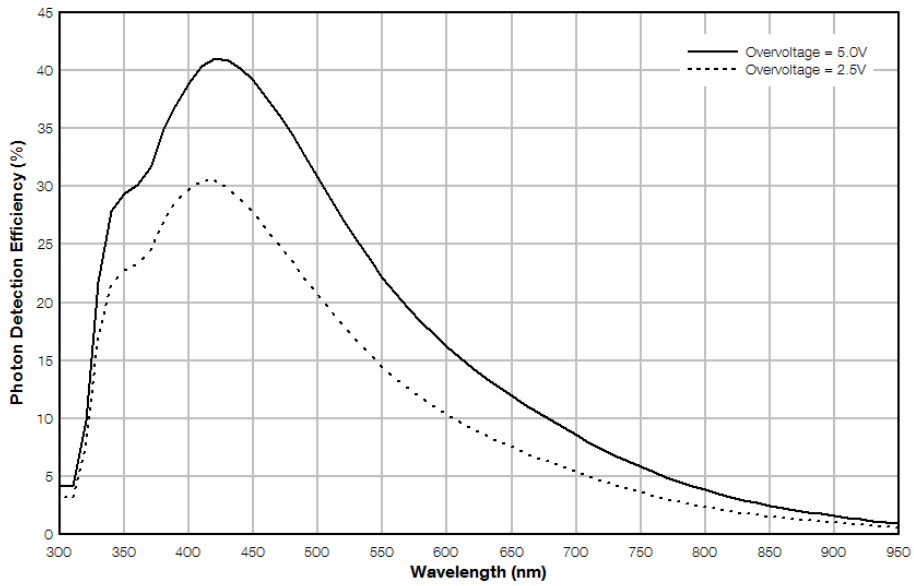


Figure 3. PDE versus Wavelength
(MicroFC-30035-SMT)

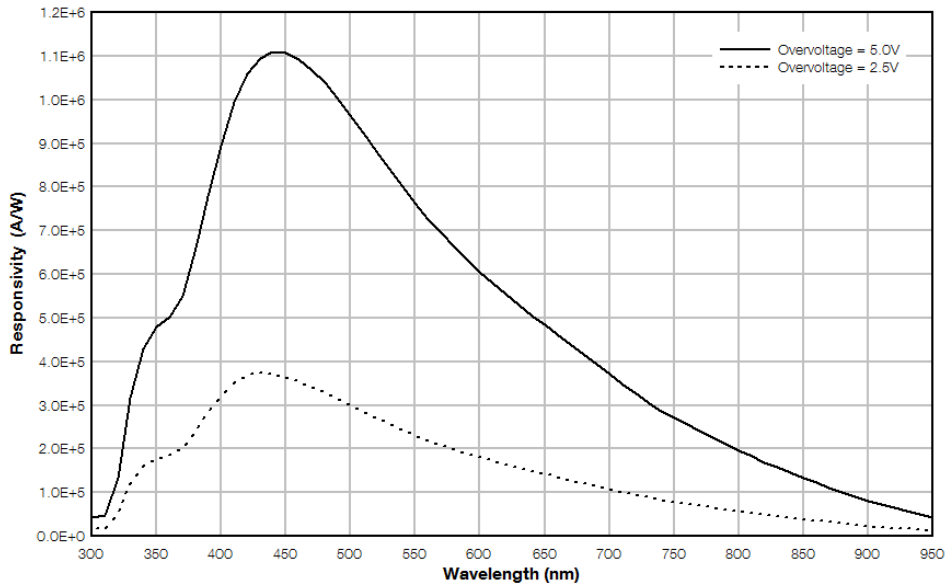


Figure 4. Responsivity versus Wavelength
(MicroFC-30035-SMT)

C-Series SiPM Sensors

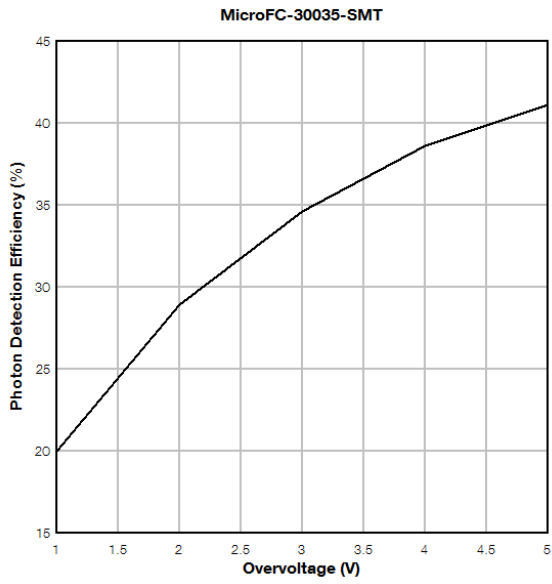


Figure 5. PDE at 420 nm versus Voltage

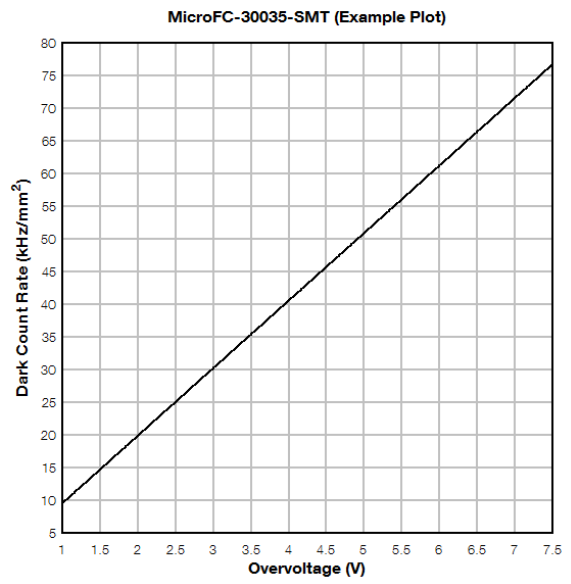


Figure 6. Dark Count Rate versus Overvoltage

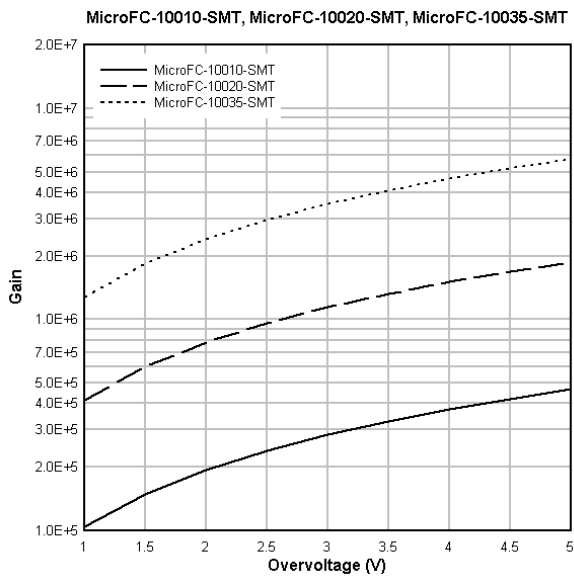


Figure 7. Gain versus Overvoltage

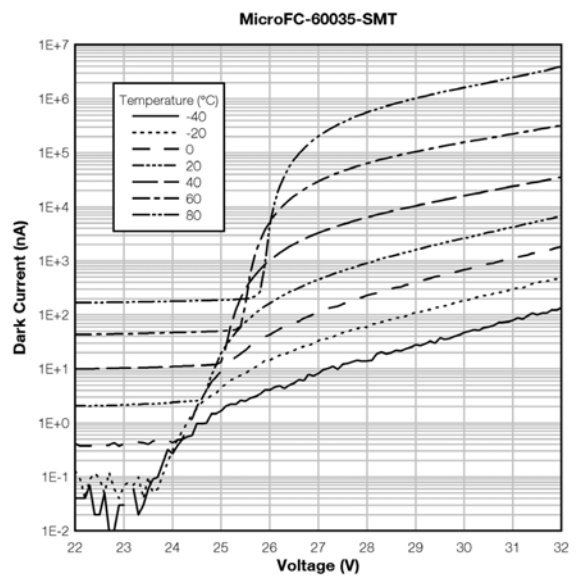


Figure 8. Dark Current versus Voltage and Temperature

C-Series SiPM Sensors

EVALUATION BOARD OPTIONS

SMA Biasing Board (MicroFC-SMA-XXXXX)

The MicroFC-SMA is a printed circuit board (PCB) that can facilitate the evaluation of the C-Series SMT sensors. The board has three female SMA connectors for connecting the bias voltage, the standard output from the anode and the fast output signal. The output signals can be connected directly to a 50 Ω -terminated oscilloscope for viewing. The biasing and output signal tracks are laid out in such a way as to preserve the fast timing characteristics of the sensor.

The MicroFC-SMA is recommended for users who require a plug-and-play set-up to quickly evaluate C-Series SMT sensors with optimum timing performance. The board also allows the standard output from the anode-cathode readout to be observed at the same time as the fast output. The outputs can be connected directly to the oscilloscope or measurement device, but external preamplification may be required to boost the signal. The table below lists the SMA board connections. The SMA board electrical schematics are available to download in [AND9809/D](#).

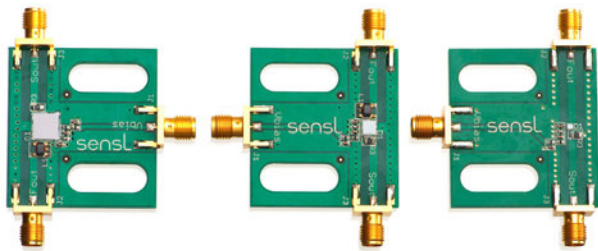


Figure 9. SMA Biasing Board

MicroFC-SMA-XXXXX	
Output	Function
Vbias	Positive bias input (cathode)
Fout	Fast output
Sout	Standard output (anode)

Pin Adapter (MicroFC-SMTPA-XXXXX)

The SMT Pin Adapter board (SMTPA) is a small PCB board that houses the SMT sensor and has through-hole pins to allow for use with standard sockets or probe clips. This product is useful for those needing a quick way to evaluate the C-Series SMT sensors without the need for specialist surface-mount soldering. While this is a 'quick fix' suitable for many evaluations, it should be noted that the timing performance from this board will not be optimized and if the best possible timing performance is required, the MicroFC-SMA-XXXXX is recommended. The pin-out

information is shown in the table below. The SMTPA board electrical schematics are shown in Figure 12 and are available to download in [AND9809/D](#).



Figure 10. Pin Adapter

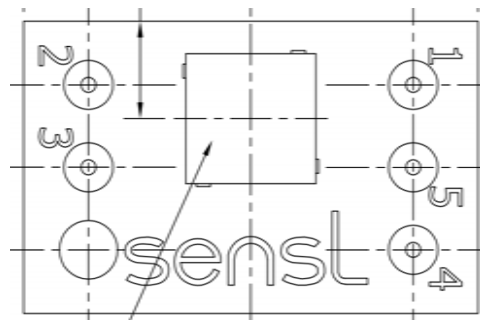


Figure 11. MicroFC-SMTPA-XXXXX

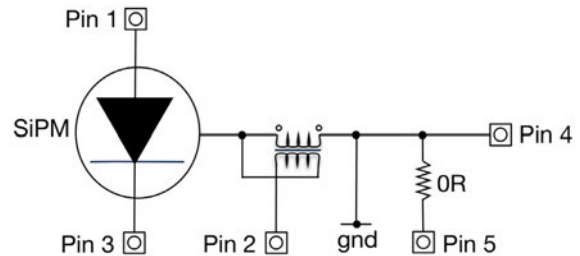


Figure 12. SMTPA Board Circuit Schematic

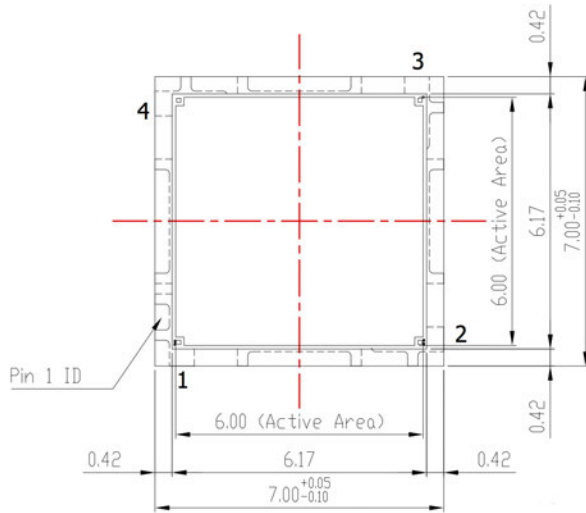
MicroFC-SMTPA-XXXXX	
Pin No.	Connection
1	Anode
2	Fast output
3	Cathode
4	Ground
5	No connect

C-Series SiPM Sensors

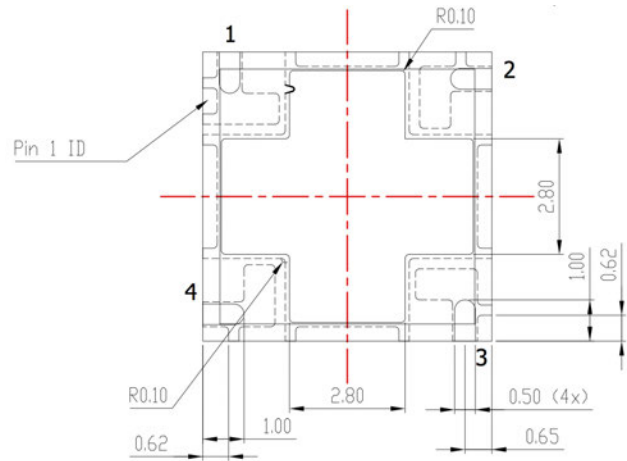
PACKAGE DIMENSIONS

(All Dimensions in mm)

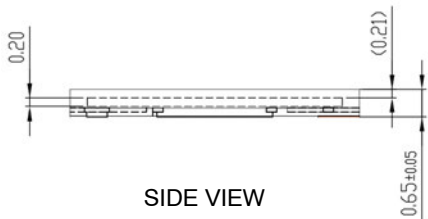
MicroFC-60035-SMT



TOP VIEW



BOTTOM VIEW



SIDE VIEW

Pin Assignments	
Pin #	MicroFC-60035-SMT
1	Anode
2	Fast Output
3	Cathode
4, 5	No Connect*

*The 'No Connect' pin 4 should be soldered to the PCB. This pin can be connected to ground but it can also be left floating without affecting the dark noise. It is recommended that the Pin 5 paddle is NOT soldered to the PCB and is left floating to achieve optimal soldering on pins 1 to 4. Please note the full advice in the CAD file.

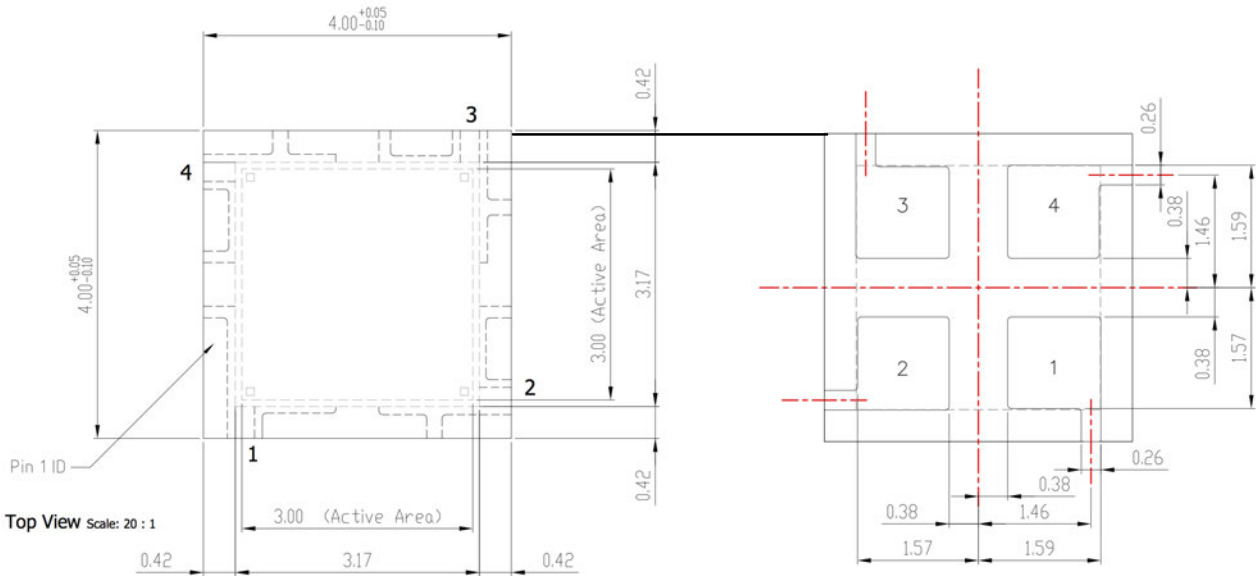
The complete MicroFC-60035-SMT CAD file, including solder footprint and tape and reel drawing, is available to download [here](#).

C-Series SiPM Sensors

PACKAGE DIMENSIONS

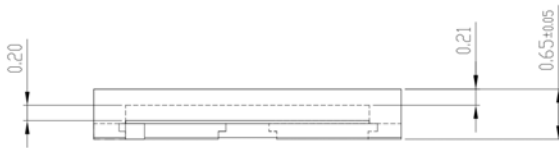
(All Dimensions in mm)

MicroFC-30035-SMT



TOP VIEW

BOTTOM VIEW



SIDE VIEW

Pin Assignments	
Pin #	MicroFC-300XX-SMT
1	Anode
2	Fast Output
3	Cathode
4	No Connect*

*The 'No Connect' pin 4 should be soldered to the PCB. It can be connected to ground but it can also be left floating without affecting the dark noise.

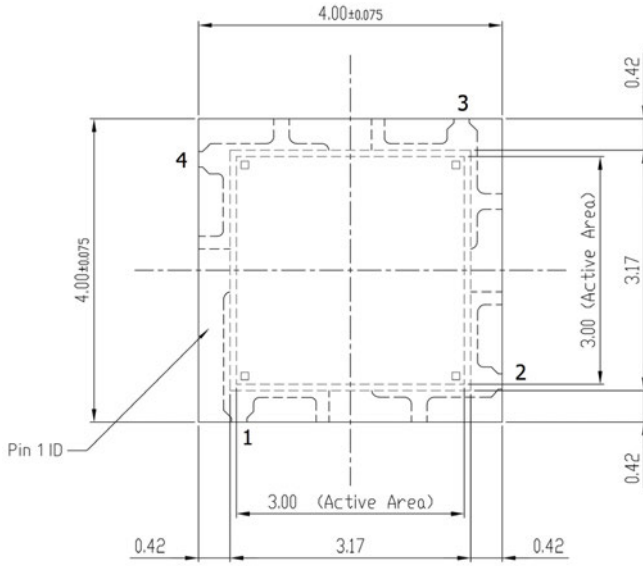
The complete MicroFC-30035-SMT CAD file, including solder footprint and tape and reel drawing, is available to download [here](#).

C-Series SiPM Sensors

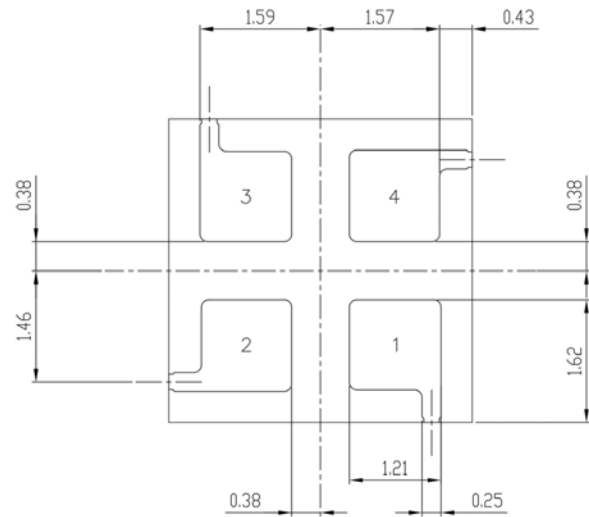
PACKAGE DIMENSIONS

(All Dimensions in mm)

MicroFC-30020-SMT & MicroFC-30050-SMT



TOP VIEW



BOTTOM VIEW



SIDE VIEW

Pin Assignments	
Pin #	MicroFC-300XX-SMT
1	Anode
2	Fast Output
3	Cathode
4	No Connect*

*The 'No Connect' pin 4 should be soldered to the PCB. It can be connected to ground but it can also be left floating without affecting the dark noise.

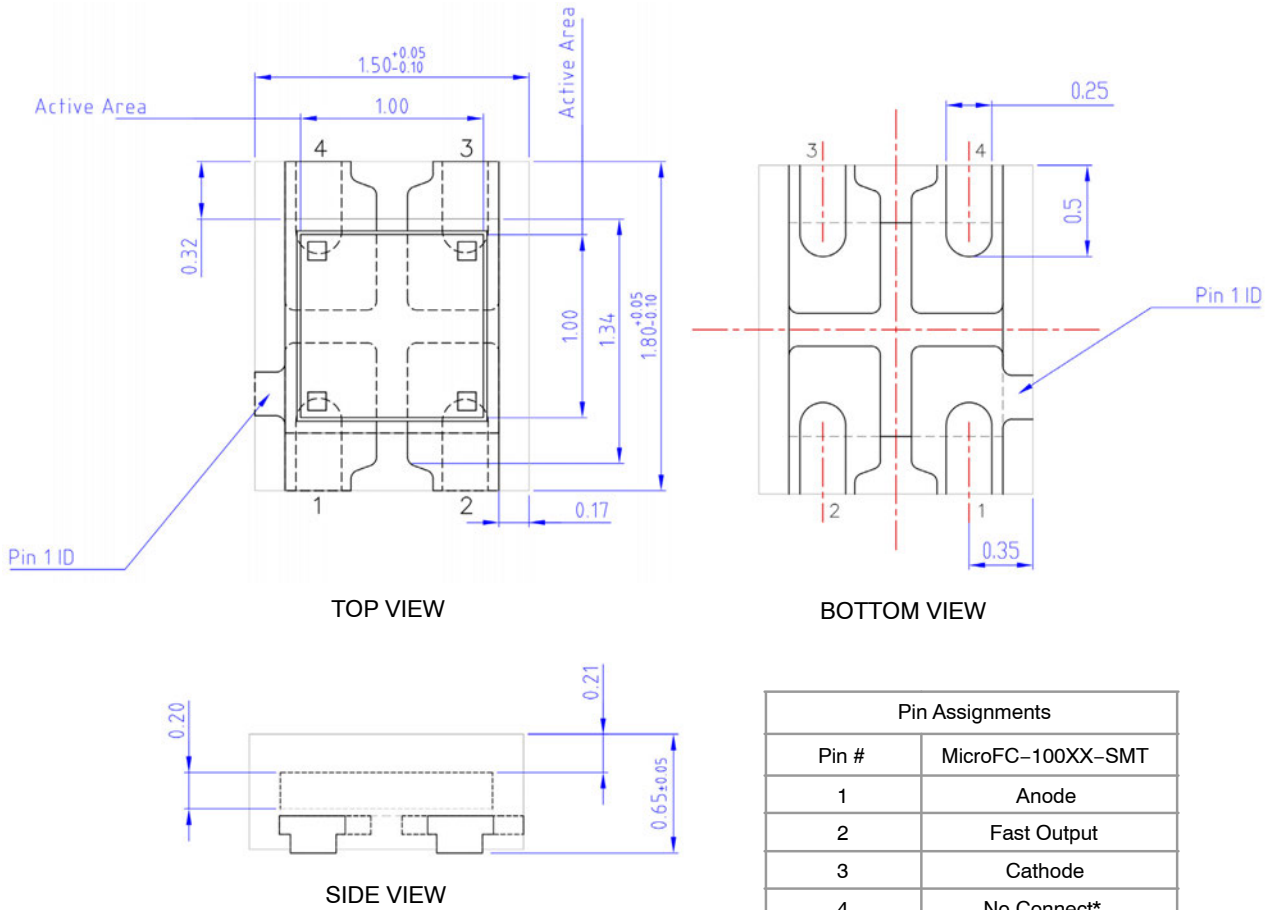
The complete MicroFC-300XX-SMT CAD and solder footprint file is available to download [here](#).

C-Series SiPM Sensors

PACKAGE DIMENSIONS

(All Dimensions in mm)

MicroFC-10010-SMT, MicroFC-10020-SMT & MicroFC-10035-SMT



*The 'No Connect' pin 4 should be soldered to the PCB. It can be connected to ground but it can also be left floating without affecting the dark noise.

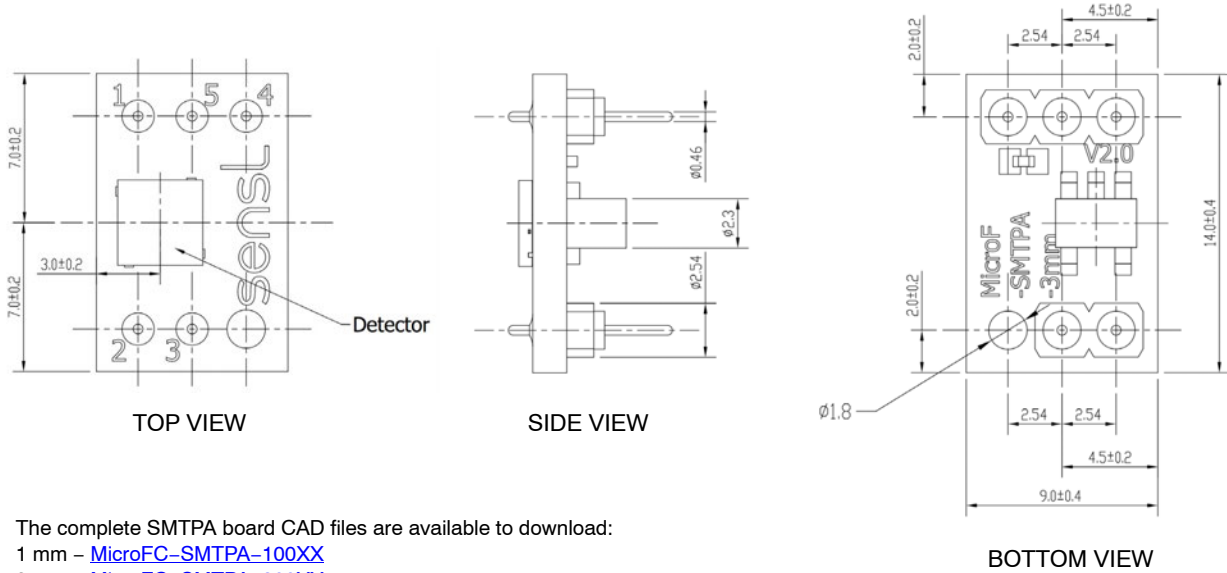
The complete MicroFC-100XX-SMT CAD and solder footprint file is available to download [here](#).

C-Series SiPM Sensors

PACKAGE DIMENSIONS

(All Dimensions in mm)

MicroFC-SMTPA Board

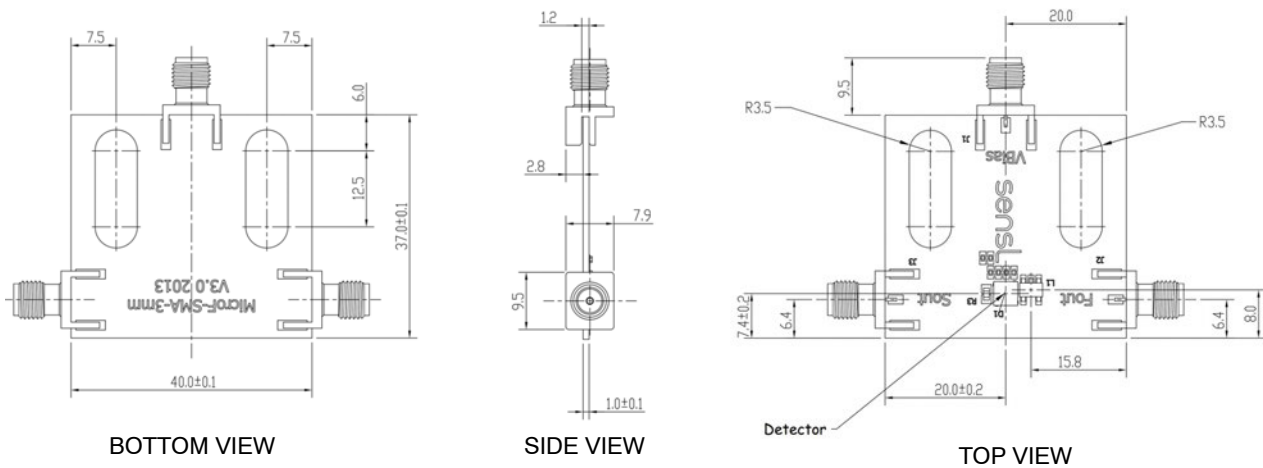


The complete SMTPA board CAD files are available to download:

- 1 mm – [MicroFC-SMTPA-100XX](#)
- 3 mm – [MicroFC-SMTPA-300XX](#)
- 6 mm – [MicroFC-SMTPA-60035](#)

The electrical schematics for the SMTPA board is available in [AND9809/D](#).

MicroFC-SMA Board



The complete SMA board CAD files are available to download:

- 1 mm – [MicroFC-SMA-100XX](#)
- 3 mm – [MicroFC-SMA-300XX](#)
- 6 mm – [MicroFC-SMA-60035](#)

The electrical schematics for the SMA board is available in [AND9809/D](#).

C-Series SiPM Sensors

USEFUL LINKS

- [Introduction to Silicon Photomultipliers Application Note](#) – If you are new to SiPM, this document explains their operation and main performance parameters.
- [Biasing and Readout Application Note](#) – This document gives detailed information on how to bias the sensor for both standard and fast configurations, and amplifying and reading out the signal.
- [How to Evaluate and Compare Silicon Photomultipliers Application Note](#) – Information on what to consider when selecting an SiPM.
- [Handling and Soldering Guide](#) – This document gives information on safe handling of the sensors and soldering to PCB.
- [ON Semiconductor Website](#) – for more information on all of ON Semiconductor’s products as well as application information.
- [CAD file library](#) – ON Semiconductor CAD files include solder footprints and tape and reel information.

ORDERING INFORMATION

Table 5. ORDERING INFORMATION

Product Code (Note 11)	Microcell Size (Total Number)	Sensor Active Area	Package Type	Delivery Options (Note 12)
10000 Series				
MICROFC-10010-SMT	10 μm (2880 microcells)	1 mm × 1 mm	4-side tileable, surface mount package (SMT)	TR1, TR
MICROFC-SMA-10010-GEVB			SMT sensor mounted onto a PCB with SMA connectors for bias and output.	PK
MICROFC-SMTPA-10010-GEVB			SMT sensor mounted onto a pin adapter board.	PK
MICROFC-10020-SMT	20 μm (1296 microcells)		4-side tileable, surface mount package (SMT)	TR1, TR
MICROFC-SMA-10020-GEVB			SMT sensor mounted onto a PCB with SMA connectors for bias and output.	PK
MICROFC-SMTPA-10020-GEVB			SMT sensor mounted onto a pin adapter board.	PK
MICROFC-10035-SMT	35 μm (576 microcells)		4-side tileable, surface mount package (SMT)	TR1, TR
MICROFC-SMA-10035-GEVB			SMT sensor mounted onto a PCB with SMA connectors for bias and output.	PK
MICROFC-SMTPA-10035-GEVB			SMT sensor mounted onto a pin adapter board.	PK

C-Series SiPM Sensors

Table 5. ORDERING INFORMATION (continued)

Product Code (Note 11)	Microcell Size (Total Number)	Sensor Active Area	Package Type	Delivery Options (Note 12)
30000 Series				
MICROFC-30020-SMT	20 μm (10998 microcells)	3 mm \times 3 mm	4-side tileable, surface mount package (SMT)	TR1, TR
MICROFC-SMA-30020-GEVB			SMT sensor mounted onto a PCB with SMA connectors for bias and output.	PK
MICROFC-SMTPA-30020-GEVB			SMT sensor mounted onto a pin adapter board	PK
MICROFC-30035-SMT	35 μm (4774 microcells)		4-side tileable, surface mount package (SMT)	TR1, TR
MICROFC-SMA-30035-GEVB			SMT sensor mounted onto a PCB with SMA connectors for bias and output.	PK
MICROFC-SMTPA-30035-GEVB			SMT sensor mounted onto a pin adapter board	PK
MICROFC-30050-SMT	50 μm (2668 microcells)		4-side tileable, surface mount package (SMT)	TR1, TR
MICROFC-SMA-30050-GEVB			SMT sensor mounted onto a PCB with SMA connectors for bias and output.	PK
MICROFC-SMTPA-30050-GEVB			SMT sensor mounted onto a pin adapter board	PK

60000 Series

MICROFC-60035-SMT	35 μm (18980 microcells)	6mm \times 6mm	4-side tileable, surface mount package (SMT)	TR1, TR
MICROFC-SMA-60035-GEVB			SMT sensor mounted onto a PCB with SMA connectors for bias and output.	PK
MICROFC-SMTPA-60035-GEVB			SMT sensor mounted onto a pin adapter board	PK

11. All Devices are Pb-Free and are RoHS Compliant.


12. The two-letter delivery option code should be appended to the order number, e.g.) to receive MICROFC-60035-SMT on tape and reel, use

MICROFC-60035-SMT-TR. The codes are as follows:

- PK = ESD Package
- TR1 = Tape
- TR = Tape and Reel

There is a minimum order quantity (MOQ) of 3000 for the tape and reel (TR) option. The TR option is only available in multiples of the MOQ.

SensL is a registered trademark of Semiconductor Components Industries, LLC (SCILLC) or its subsidiaries in the United States and/or other countries.

ON Semiconductor and  are trademarks of Semiconductor Components Industries, LLC dba ON Semiconductor or its subsidiaries in the United States and/or other countries. ON Semiconductor owns the rights to a number of patents, trademarks, copyrights, trade secrets, and other intellectual property. A listing of ON Semiconductor's product/patent coverage may be accessed at www.onsemi.com/site/pdf/Patent-Marking.pdf. ON Semiconductor reserves the right to make changes without further notice to any products herein. ON Semiconductor makes no warranty, representation or guarantee regarding the suitability of its products for any particular purpose, nor does ON Semiconductor assume any liability arising out of the application or use of any product or circuit, and specifically disclaims any and all liability, including without limitation special, consequential or incidental damages. Buyer is responsible for its products and applications using ON Semiconductor products, including compliance with all laws, regulations and safety requirements or standards, regardless of any support or applications information provided by ON Semiconductor. "Typical" parameters which may be provided in ON Semiconductor data sheets and/or specifications can and do vary in different applications and actual performance may vary over time. All operating parameters, including "Typicals" must be validated for each customer application by customer's technical experts. ON Semiconductor does not convey any license under its patent rights nor the rights of others. ON Semiconductor products are not designed, intended, or authorized for use as a critical component in life support systems or any FDA Class 3 medical devices or medical devices with a same or similar classification in a foreign jurisdiction or any devices intended for implantation in the human body. Should Buyer purchase or use ON Semiconductor products for any such unintended or unauthorized application, Buyer shall indemnify and hold ON Semiconductor and its officers, employees, subsidiaries, affiliates, and distributors harmless against all claims, costs, damages, and expenses, and reasonable attorney fees arising out of, directly or indirectly, any claim of personal injury or death associated with such unintended or unauthorized use, even if such claim alleges that ON Semiconductor was negligent regarding the design or manufacture of the part. ON Semiconductor is an Equal Opportunity/Affirmative Action Employer. This literature is subject to all applicable copyright laws and is not for resale in any manner.

PUBLICATION ORDERING INFORMATION

LITERATURE FULFILLMENT:

Literature Distribution Center for ON Semiconductor
 19521 E. 32nd Pkwy, Aurora, Colorado 80011 USA
Phone: 303-675-2175 or 800-344-3860 Toll Free USA/Canada
Fax: 303-675-2176 or 800-344-3867 Toll Free USA/Canada
Email: orderlit@onsemi.com

N. American Technical Support: 800-282-9855 Toll Free
 USA/Canada

Europe, Middle East and Africa Technical Support:
 Phone: 421 33 790 2910

ON Semiconductor Website: www.onsemi.com

Order Literature: <http://www.onsemi.com/orderlit>

For additional information, please contact your local Sales Representative

